REPORT DOCUMENTATION PAGE

Form Approved OMB NO. 0704-0188

The public reporting burden for this collection of information is estimated to average 1 hour per response, including the time for reviewing instructions, searching existing data sources, gathering and maintaining the data needed, and completing and reviewing the collection of information. Send comments regarding this burden estimate or any other aspect of this collection of information, including suggesstions for reducing this burden, to Washington Headquarters Services, Directorate for Information Operations and Reports, 1215 Jefferson Davis Highway, Suite 1204, Arlington VA, 22202-4302. Respondents should be aware that notwithstanding any other provision of law, no person shall be subject to any oenalty for failing to comply with a collection of information if it does not display a currently valid OMB control number.
PLEASE DO NOT RETURN YOUR FORM TO THE ABOVE ADDRESS.

1. REPORT DATE (DD-MM-YYYY)	2. REPORT TYPE	3. DATES COVERED (From - To)
16-05-2022	Final Report	1-Nov-2017 - 30-Jun-2021

4. TITLE AND SUBTITLE

Final Report: Disruptive Approaches to Energetic Material Synthesis: Nanosecond Cold Liquid Plasma (NCLP) for the Synthesis of New Nitrogen Polymers and Other Novel Nitrogen-based Materials

5a. CONTRACT NUMBER
W911NF-17-1-0597

5b. GRANT NUMBER

5c. PROGRAM ELEMENT NUMBER
611102

6. AUTHORS

5d. PROJECT NUMBER

5e. TASK NUMBER

5f. WORK UNIT NUMBER

7. PERFORMING ORGANIZATION NAMES AND ADDRESSES

Drexel University
Office of Research
3201 Arch Street, Suite 100
Philadelphia, PA 19104 -2875

8. PERFORMING ORGANIZATION REPORT NUMBER

9. SPONSORING/MONITORING AGENCY NAME(S) AND ADDRESS (ES)

U.S. Army Research Office
P.O. Box 12211
Research Triangle Park, NC 27709-2211

10. SPONSOR/MONITOR'S ACRONYM(S)
ARO

11. SPONSOR/MONITOR'S REPORT NUMBER(S)
71327-CH.13

12. DISTRIBUTION AVAILIBILITY STATEMENT

Approved for public release; distribution is unlimited.

13. SUPPLEMENTARY NOTES

The views, opinions and/or findings contained in this report are those of the author(s) and should not contrued as an official Department of the Army position, policy or decision, unless so designated by other documentation.

14. ABSTRACT

15. SUBJECT TERMS

16. SECURITY CLASSIFICATION OF:			17. LIMITATION OF ABSTRACT	15. NUMBER OF PAGES	19a. NAME OF RESPONSIBLE PERSON
a. REPORT	b. ABSTRACT	c. THIS PAGE			Danil Dobrynin
UU	UU	UU	UU		19b. TELEPHONE NUMBER 215-895-6254

RPPR Final Report
as of 06-Jun-2022

Agency Code: 21XD

Proposal Number: 71327CH **Agreement Number: W911NF-17-1-0597**
INVESTIGATOR(S):

Name: Alexander Fridman
Email: alexander.fridman@drexel.edu
Phone Number: 2158951542
Principal: N

Name: Danil Dobrynin
Email: dvd34@drexel.edu
Phone Number: 2158956254
Principal: Y

Organization: **Drexel University**
Address: Office of Research, Philadelphia, PA 191042875
Country: USA
DUNS Number: 002604817 EIN: 231352630

Report Date: 30-Sep-2021 Date Received: 16-May-2022
Final Report for Period Beginning 01-Nov-2017 and Ending 30-Jun-2021

Title: Disruptive Approaches to Energetic Material Synthesis: Nanosecond Cold Liquid Plasma (NCLP) for the Synthesis of New Nitrogen Polymers and Other Novel Nitrogen-based Materials
Begin Performance Period: 01-Nov-2017 **End Performance Period:** 30-Jun-2021
Report Term: 0-Other

Submitted By: Danil Dobrynin Email: dvd34@drexel.edu
Phone: (215) 895-6254

Distribution Statement: 1-Approved for public release; distribution is unlimited.

STEM Degrees: **STEM Participants:** 2

Major Goals: The project objective is to explore the possibility and fundamental science of the synthesis of nitrogen polymers and other novel nitrogen-based materials using fundamentally new phenomenon of nanosecond-pulsed cold liquid plasma (NCLP). Recently discovered new physical process of NCLP is a phenomenon of direct ionization of liquid phase by sharp high electric field pulses without heating. The proposed NCLP technique will potentially allow the generation of metastable (or possibly stable at ambient conditions) new energetic materials which are currently unrecoverable.
This project is intended to answer the following fundamental questions: What are the materials that can be synthesized using nanosecond-pulsed plasma in liquid nitrogen? What are the physio-chemical conditions required for this synthesis? What are the chemical and physical characteristics of these materials? How can these materials be stabilized to be recovered at normal conditions? What are the scalability restrictions and how we would be able to mitigate them?
In order to characterize the obtained materials, we intend to utilize several techniques available on site: optical spectroscopy, gas and liquid phase FTIR (analysis of liquid phase composition, if possible, and products of reactions in gas phase, for example, generation of NOx species in reaction with pure oxygen), and colorimetry. Further analysis of these compounds to be continued by ARL using a variety of characterization techniques from x-ray diffraction and optical spectroscopy, to differential scanning calorimetry and other energetic characterization techniques, such as burn rate measurements and formulation studies. In order to examine the stability of produced materials, we explore the possibilities of (a) passivation of terminal ends with hydrogen (for example, by adding hydrogen-containing compounds directly into liquid nitrogen (azanes, azenes)); and (b) incorporation of the produced material into porous media (silicone or carbon).
Experimental goals are formulated as follows:
1. To develop an experimental setup for generation of nanosecond-pulsed plasma in liquid nitrogen
2. Perform optical diagnostics of nanosecond-pulsed discharge in liquid nitrogen
3. To characterize the materials generated in liquid nitrogen plasma using Raman spectroscopy and FTIR analysis of gaseous products. Further analysis of these compounds to be continued by ARL using a variety of characterization techniques from x-ray diffraction and optical spectroscopy, to differential scanning calorimetry and other energetic characterization techniques, such as burn rate measurements and formulation studies.

4. To investigate possible product stabilization pathways.

Accomplishments: Goal 1: Two systems were developed and tested. One is based on nanosecond-pulsed spark discharge in LN, the second - on nanosecond-pulsed corona discharge in LN. Dark (black/dark brown) product was generated in both systems. Plasma-generated product rapid decomposition upon heating in both air and nitrogen atmospheres was observed (see reports 1 and 2 for periods of November 1, 2017 – July 31, 2018 and August 1, 2019 – July 31, 2020)

Goal 2: Detailed optical characterization of the discharge has been performed. Results on the discharge integral and time resolved imaging and temperature measurements were obtained. Nanosecond-pulsed discharge in liquid nitrogen, much like in water, initially ignites directly in liquid phase, and energy release eventually results in generation of gaseous voids. First temperature estimations from the molecular nitrogen emission shows maximum temperature increase on the order of 60 K which is advantageous for non-thermal material synthesis in liquid phase (see report 2 for period of August 1, 2019 – July 31, 2020).

Goal 3: Raman measurements of the materials (in pure LN and using NaN3 as a precursor) were obtained, as well as FTIR characterization of gas phase products. We have observed production of nitrogen-based material in this discharge which preliminarily can be identified as a form of energetic non-molecular nitrogen compound due to the following reasons: a) no electrode erosion was observed while amount of produced material was significant; b) material decomposition, accompanied by light and sound wave generation, was triggered by heating; c) no residue was left after the decomposition; and d) absence of NOx species, except N2O, in the reaction products as registered by FTIR indicates low-temperature decomposition mechanism (see also report 2 for period of August 1, 2019 – July 31, 2020). Experiments with production of polynitrogen compounds from potassium azide revealed synthesis of K2N6, with planar N6 rings and K- ions having P6/mmm symmetry. The mechanism of such transformation was determined as being in contact with the spark discharge, that is, due to the highly unstable short life active species formed in plasma channel in combination with high temperature of the nanosecond-pulsed spark discharge itself.

Goal 4: Experiments of plasma ignition in liquid nitrogen in presence of sodium azide (NaN3) were performed. Experimental characterization techniques show that plasma treatment of NaN3 results in production of colored material with spectral characteristics close to N6 polynitrogen compounds, although it is most likely is a mixture of different compounds. We also report that the obtained material appears to be stable at ambient pressure at temperatures up to around -55 ºC. We also followed Raman peaks of the produced material while placed on solid CO2 and show that it is stable for at least 30 minutes. Additional experiments with several other precursors/stabilizing agents were performed, showing that some of them (activated carbon, boron nitrate nanotubes and magnesium) allow generation of other nitrogen-based unstable products.

In another set of experiments, LN was treated in presence of activated carbon (used as porous media for preservation/stabilization). After the treatment, a highly unstable, shock- and temperature-sensitive material embedded into carbon was produced. Experimental measurements of the material explosive decomposition by shadow imaging of generated shockwaves indicate that the material energy density is ~12±4 kJ/g, almost 3 times that of TNT and close to predicted energy density of cg-N. treatment of liquid nitrogen demonstrating synthesis of a highly energetic nitrogen material. Raman, FTIR analysis of gas phase products of decomposition, and the material explosion characteristics suggest synthesis of polymeric (amorphous) nitrogen compound which is stable at ambient pressure up to temperatures of about -150 C. Addition of adsorbents with relatively large characteristic pore sizes (>5 nm) allows marginally improved recovery of the material as determined by temperature-dependent Raman measurements.

Training Opportunities: 2 graduate PhD students participated in the project
1 high school student participated as an intern learning about plasmas, polynitrogen compounds and chemistry. Participation was limited to learning and observations of experiments.

Results Dissemination: The results were published in 3 peer-reviewed jounals, presented in several major international conferences (APS Gaseous electronics conferences 2019-2021, International conference on plasma science 2019, Materials research symposium 2019, Pulsed power and plasma science 2019). The results were also broadly disseminated in a Drexel University press release (picked up by several news outlets worldwide, as well as public forums like Reddit) and published in Drexel University Magazine EXEL in 2020: https://exelmagazine.org/article/liquid-plasma-fuels-a-breakthrough/.

RPPR Final Report
as of 06-Jun-2022

Honors and Awards: Nothing to Report

Protocol Activity Status:

Technology Transfer: Patent titled "METHOD FOR GENERATION OF NOVEL MATERIALS USING NANOSECOND-PULSED DISCHARGE PLASMA IN LIQUID PHASE" was filled:

U.S. Provisional Patent Application No. 62/871,052
For: Methoed for Generation of Novel Materials Using Nanosecond-Pulsed Discharge Plasma in Liquid Phase
Drexel Docket No. 19-2251 - MD Ref: DREX-1220USP

PARTICIPANTS:

Participant Type: PD/PI
Participant: Danil Dobrynin
Person Months Worked: 3.00 **Funding Support:**
Project Contribution:
National Academy Member: N

Participant Type: Co PD/PI
Participant: Alexander Fridman
Person Months Worked: 1.00 **Funding Support:**
Project Contribution:
National Academy Member: Y

Participant Type: Graduate Student (research assistant)
Participant: Zhihen Song
Person Months Worked: 12.00 **Funding Support:**
Project Contribution:
National Academy Member: N

Participant Type: Graduate Student (research assistant)
Participant: Roman Rakhmanov
Person Months Worked: 12.00 **Funding Support:**
Project Contribution:
National Academy Member: N

Participant Type: High School Student
Participant: Jacob Cho
Person Months Worked: 1.00 **Funding Support:**
Project Contribution:
National Academy Member: N

RPPR Final Report
as of 06-Jun-2022

ARTICLES:

Publication Type: Journal Article Peer Reviewed: Y **Publication Status:** 1-Published
Journal: Journal of Physics D: Applied Physics
Publication Identifier Type: DOI Publication Identifier: 10.1088/1361-6463/ab30f1
Volume: 52 Issue: 39 First Page #:
Date Submitted: 8/27/19 12:00AM Date Published: 9/1/19 4:00AM
Publication Location:
Article Title: Nanosecond-pulsed discharge in liquid nitrogen: optical characterization and production of an energetic non-molecular form of nitrogen-rich material
Authors: Danil Dobrynin, Roman Rakhmanov, Alexander Fridman
Keywords: nanosecondpulsed plasma in liquid nitrogen
Abstract: Nanosecond-pulsed discharge in liquid nitrogen ignited using a needle electrode and positive 60?kV high voltage pulses was characterized using fast and shadow imaging, as well as optical emission spectroscopy. Estimation of temperature was done using molecular nitrogen emission of second positive system ro-vibrational transition spectra, and the maximum temperature increase is estimated to be ~60?K. We also report on the first observations of plasma-generated unstable material from liquid nitrogen, presumably a form of polynitrogen compound.
Distribution Statement: 3-Distribution authorized to U.S. Government Agencies and their contractors
Acknowledged Federal Support: **Y**

Publication Type: Journal Article Peer Reviewed: Y **Publication Status:** 1-Published
Journal: Journal of Physics D: Applied Physics
Publication Identifier Type: DOI Publication Identifier: 10.1088/1361-6463/ab349a
Volume: 52 Issue: 45 First Page #: 455502
Date Submitted: 8/27/19 12:00AM Date Published: 11/1/19 4:00AM
Publication Location:
Article Title: Nanosecond-pulsed spark discharge plasma in liquid nitrogen: synthesis of polynitrogen from NaN
Authors: Danil Dobrynin, Roman Rakhmanov, Alexander Fridman
Keywords: nanosecond spark discharge, plasma in liquid nitrogen
Abstract: Nanosecond-pulsed plasma ignited in liquid nitrogen is a unique tool for the synthesis of unconventional materials due to a combination of energetic properties of the discharge itself (high densities of reactive species, pressures and radiation) with the low temperature of the surrounding dense liquid. Here, we report on applications of such plasma for synthesis of a polymeric nitrogen compound, preliminarily identified as neutral or ionic N6, from sodium azide precursors.
Distribution Statement: 3-Distribution authorized to U.S. Government Agencies and their contractors
Acknowledged Federal Support: **Y**

RPPR Final Report
as of 06-Jun-2022

Publication Type: Journal Article Peer Reviewed: Y **Publication Status:** 1-Published
Journal: Materials
Publication Identifier Type: DOI Publication Identifier: 10.3390/ma14154292
Volume: 14 Issue: 15 First Page #: 4292
Date Submitted: 5/16/22 12:00AM Date Published: 7/1/21 8:00AM
Publication Location:
Article Title: Synthesis of Highly Energetic PolyNitrogen by Nanosecond-Pulsed Plasma in Liquid Nitrogen
Authors: Danil Dobrynin, Zhiheng Song, Alexander Fridman
Keywords: nanosecond plasma in liquid; polymeric nitrogen; energetic materials
Abstract: We report on an experimental study of nanosecond-pulsed plasma treatment of liquid nitrogen demonstrating synthesis of a highly energetic nitrogen material. Raman, FTIR analysis of gas phase products of decomposition, and the material explosion characteristics suggest synthesis of polymeric (amorphous) nitrogen compound which is stable at ambient pressure up to temperatures of about ?150 °C. Addition of adsorbents with relatively large characteristic pore sizes (>5 nm) allows marginally improved recovery of the material as determined by temperature-dependent Raman measurements. By analyzing the shock wave propagation resulting from the explosions, we estimated the energy density of the material to be 13.3 ± 3.5 kJ/g, close to the previously predicted value for amorphous polymeric nitrogen.
Distribution Statement: 2-Distribution Limited to U.S. Government agencies only; report contains proprietary info
Acknowledged Federal Support: **Y**

Publication Type: Journal Article Peer Reviewed: Y **Publication Status:** 0-Other
Journal: not published
Publication Identifier Type: Publication Identifier:
Volume: Issue: First Page #:
Date Submitted: 5/16/22 12:00AM Date Published:
Publication Location:
Article Title: In-liquid nanosecond-pulsed spark discharge plasma: Synthesis of polynitrogen from potassium azide in liquid nitrogen
Authors: Zhiheng Song, Alexander Fridman, Danil Dobrynin
Keywords: liquid nitrogen plasma, liquid plasma, nanosecond-pulsed discharge, potassium azide, polynitrogen
Abstract: Here we report a method about synthesis of polynitrogen materials by nanosecond-pulsed spark discharge plasma under liquid nitrogen. The polynitrogen material was synthesized from potassium azide, preliminarily characterized by Raman and FTIR spectroscopy, as K2N6, with planar N6 rings and K- ions having P6/mmm symmetry. The mechanism of such transformation was determined as being in contact with the spark discharge, that is, due to the highly unstable short life active species formed in plasma channel in combination with high temperature of the nanosecond-pulsed spark discharge itself.
Distribution Statement: 2-Distribution Limited to U.S. Government agencies only; report contains proprietary info
Acknowledged Federal Support: **Y**

CONFERENCE PAPERS:

Publication Type: Conference Paper or Presentation **Publication Status:** 1-Published
Conference Name: The 45th IEEE International Conference on Plasma Science (ICOPS 2018)
Date Received: 27-Aug-2019 Conference Date: 29-Jun-2018 Date Published:
Conference Location: Denver, CO
Paper Title: NANOSECOND-PULSED DISCHARGE IN LIQUID NITROGEN
Authors: Danil Dobrynin, Roman Rakhmanov, Alexander Fridman
Acknowledged Federal Support: **Y**

RPPR Final Report
as of 06-Jun-2022

Publication Type: Conference Paper or Presentation **Publication Status:** 1-Published
Conference Name: 2018 MRS Fall Meeting & Exhibit
Date Received: 27-Aug-2019 Conference Date: 01-Dec-2018 Date Published:
Conference Location: Boston, MA
Paper Title: Nanosecond-Pulsed Cold Plasma in Liuqid Nitrogen for the Synthesis of Nitrogen-based Materials
Authors: Danil Dobrynin, Roman Rakhmanov, Alexander Fridman
Acknowledged Federal Support: **Y**

Publication Type: Conference Paper or Presentation **Publication Status:** 1-Published
Conference Name: Pulsed power and plasma science (PPPS-2019), 46th annual ICOPS
Date Received: 27-Aug-2019 Conference Date: 23-Jun-2019 Date Published:
Conference Location: Orlando, FL
Paper Title: Nanosecond-pulsed corona discharge in liquid nitrogen and production of nitrogen polymers
Authors: Danil Dobrynin, Roman Rakhmanov, Alexander Fridman
Acknowledged Federal Support: **Y**

Publication Type: Conference Paper or Presentation **Publication Status:** 0-Other
Conference Name: Gaseous electronics conference
Date Received: 16-May-2022 Conference Date: 05-Oct-2018 Date Published:
Conference Location: Portland, Oregon, USA
Paper Title: Synthesis of nitrogen-based materials using nanosecond-pulsed plasma in liquid nitrogen
Authors: Danil Dobrynin, Roman Rakhmanov, Alexander Fridman
Acknowledged Federal Support: **Y**

WEBSITES:

URL: https://drexel.edu/news/archive/2019/november/plasma-polymeric-nitrogen
Date Received: 16-May-2022
Title: From a Cloud of Cold and a Spark, Drexel Researchers Create and Stabilize Pure Polymeric Nitrogen for the First Time
Description: News article
URL: https://exelmagazine.org/article/liquid-plasma-fuels-a-breakthrough/
Date Received: 16-May-2022
Title: Liquid plasma fuels breakthrough
Description: News article

PATENTS:

Intellectual Property Type: Patent Date Received: **16-May-2022**
Patent Title: METHOD FOR GENERATION OF NOVEL MATERIALS USING NANOSECOND-PULSED DISCHARGE PLASMA IN LIQUID PHASE
Patent Abstract:
Patent Number: US2021106968A1
Patent Country: USA
Application Date: 07-Jul-2020 Application Status: 2
Date Issued:

RPPR Final Report
as of 06-Jun-2022

Partners

,

I certify that the information in the report is complete and accurate:
Signature: Danil Dobrynin
Signature Date: 5/16/22 4:04PM

FINAL REPORT

Nanosecond Cold Liquid Plasma (NCLP) for the Synthesis of New Nitrogen Polymers and Other Novel Nitrogen-based Materials

PI: Danil Dobrynin, Co-PI: Alexander Fridman
Nyheim Plasma Institute, Drexel University

1. Introduction: objective, goals of the project and accomplishments to date

The project objective is to explore the possibility and fundamental science of the synthesis of nitrogen polymers and other novel nitrogen-based materials using fundamentally new phenomenon of nanosecond-pulsed cold liquid plasma (NCLP). Recently discovered new physical process of NCLP is a phenomenon of direct ionization of liquid phase by sharp high electric field pulses without heating. The proposed NCLP technique will potentially allow the generation of metastable (or possibly stable at ambient conditions) new energetic materials which are currently unrecoverable.

This project is intended to answer the following fundamental questions: What are the materials that can be synthesized using nanosecond-pulsed plasma in liquid nitrogen? What are the physio-chemical conditions required for this synthesis? What are the chemical and physical characteristics of these materials? How can these materials be stabilized to be recovered at normal conditions? What are the scalability restrictions and how we would be able to mitigate them?

In order to characterize the obtained materials, we intend to utilize several techniques available on site: optical spectroscopy, gas and liquid phase FTIR (analysis of liquid phase composition, if possible, and products of reactions in gas phase, for example, generation of NOx species in reaction with pure oxygen), and colorimetry. Further analysis of these compounds to be continued by ARL using a variety of characterization techniques from x-ray diffraction and optical spectroscopy, to differential scanning calorimetry and other energetic characterization techniques, such as burn rate measurements and formulation studies. In order to examine the stability of produced materials, we explore the possibilities of (a) passivation of terminal ends with hydrogen (for example, by adding hydrogen-containing compounds directly into liquid nitrogen (azanes, azenes)); and (b) incorporation of the produced material into porous media (silicone or carbon).

Experimental goals are formulated as follows:

1. To develop an experimental setup for generation of nanosecond-pulsed plasma in liquid nitrogen

2. Perform optical diagnostics of nanosecond-pulsed discharge in liquid nitrogen

3. To characterize the materials generated in liquid nitrogen plasma using Raman spectroscopy and FTIR analysis of gaseous products. Further analysis of these compounds to be continued by ARL using a variety of characterization techniques from x-ray diffraction and optical spectroscopy, to differential scanning calorimetry and other energetic characterization techniques, such as burn rate measurements and formulation studies.

4. To investigate possible product stabilization pathways.

Major accomplishments:

Goal 1: Two systems were developed and tested. One is based on nanosecond-pulsed spark discharge in LN, the second - on nanosecond-pulsed corona discharge in LN. Dark (black/dark brown) product was generated in both systems. Plasma-generated product rapid decomposition upon heating in both air and nitrogen atmospheres was observed (see reports 1 and 2 for periods of November 1, 2017 – July 31, 2018 and August 1, 2019 – July 31, 2020)

Goal 2: Detailed optical characterization of the discharge has been performed. Results on the discharge integral and time resolved imaging and temperature measurements were obtained. Nanosecond-pulsed discharge in liquid nitrogen, much like in water, initially ignites directly in liquid phase, and energy release eventually results in generation of gaseous voids. First temperature estimations from the molecular nitrogen emission shows maximum temperature increase on the order of 60 K which is advantageous for non-thermal material synthesis in liquid phase (see report 2 for period of August 1, 2019 – July 31, 2020).

Goal 3: Raman measurements of the materials (in pure LN and using NaN3 as a precursor) were obtained, as well as FTIR characterization of gas phase products. We have observed production of nitrogen-based material in this discharge which preliminarily can be identified as a form of energetic non-molecular nitrogen compound due to the following reasons: a) no electrode erosion was observed while amount of produced material was significant; b) material decomposition, accompanied by light and sound wave generation, was triggered by heating; c) no residue was left after the decomposition; and d) absence of NOx species, except N2O, in the reaction products as registered by FTIR indicates low-temperature decomposition mechanism (see also report 2 for period of August 1, 2019 – July 31, 2020). Experiments with production of polynitrogen compounds from potassium azide revealed synthesis of K2N6, with planar N6 rings and K- ions having P6/mmm symmetry. The mechanism of such transformation was determined as being in contact with the spark discharge, that is, due to the highly unstable short life active species formed in plasma channel in combination with high temperature of the nanosecond-pulsed spark discharge itself.

Goal 4: Experiments of plasma ignition in liquid nitrogen in presence of sodium azide (NaN3) were performed. Experimental characterization techniques show that plasma treatment of NaN3 results in production of colored material with spectral characteristics close to N6 polynitrogen compounds, although it is most likely is a mixture of different compounds. We also report that the obtained material appears to be stable at ambient pressure at temperatures up to around -55 ºC. We also followed Raman peaks of the produced material while placed on solid CO2 and show that it is stable for at least 30 minutes. Additional experiments with several other precursors/stabilizing agents were performed, showing that some of them (activated carbon, boron nitrate nanotubes and magnesium) allow generation of other nitrogen-based unstable products.

In another set of experiments, LN was treated in presence of activated carbon (used as porous media for preservation/stabilization). After the treatment, a highly unstable, shock- and temperature-sensitive material embedded into carbon was produced. Experimental measurements of the material explosive decomposition by shadow imaging of generated shockwaves indicate that the material energy density is ~12±4 kJ/g, almost 3 times that of TNT and close to predicted energy density of cg-N. treatment of liquid nitrogen demonstrating synthesis of a highly energetic nitrogen material. Raman, FTIR analysis of gas phase products of decomposition, and the material explosion characteristics suggest synthesis of polymeric (amorphous) nitrogen compound which is stable at ambient pressure up to temperatures of about -150 C. Addition of adsorbents with relatively large characteristic pore sizes (>5 nm) allows marginally improved recovery of the material as determined by temperature-dependent Raman measurements.

2. Experimental setups for generation of nanosecond-pulsed plasma in liquid nitrogen

To initiate the discharge in liquid nitrogen we used nanosecond pulsed power system. Two discharge cells were developed to study fundamentally different plasma modes: nanosecond-pulsed spark discharge and highly non-equilibrium nanosecond-pulsed corona discharge.

For generation of corona discharge in liquid nitrogen, a sharp (75 μm radius of curvature) tungsten electrode (Microprobes, USA) was placed in liquid nitrogen contained in 450 ml double-walled glass flask (Figure 1). The flask was fixed inside of an evacuated metal chamber to decrease liquid nitrogen evaporation rate and to screen electromagnetic noise generated by plasma. Vacuum flask was also closed from the top by a plastic lid with 3 mm diameter venting hole to minimize liquid nitrogen contamination by the surrounding air, especially oxygen. Medical grade (99% N2, O2 not more than 1.0%, CO2 <0.001%) liquid nitrogen in all experiments was purchased from Airgas, USA. High voltage tungsten electrode was powered by FPG 120-01NM10 nanosecond-pulsed power supply (FID Tech., Germany) capable of providing high voltage pulses with the parameters specified in Table 1 and the typical pulse waveform is shown in Figure 2. Typically, the corona discharge was ignited using HV pulses with amplitude of 60 kV and 20 Hz repetition frequency.

Table 1. Specifications of the FPG 120-01NM10 nanosecond-pulsed power supply

Maximum amplitude	120 kV into 50 Ohm coaxial cable
Amplitude adjustment	40 - 120 kV
Polarity	positive
Output connector	FC52-type, female – oil-filled
Rise time 10% to 90% of amplitude	less than 1-1.2 ns
Pulse duration at 90% of amplitude	8-10 ns (fixed), triangular
Maximum repetition frequency	100 Hz (adjustable)
Triggering	Internal and external
Timing jitter	less than 200 ps RMS

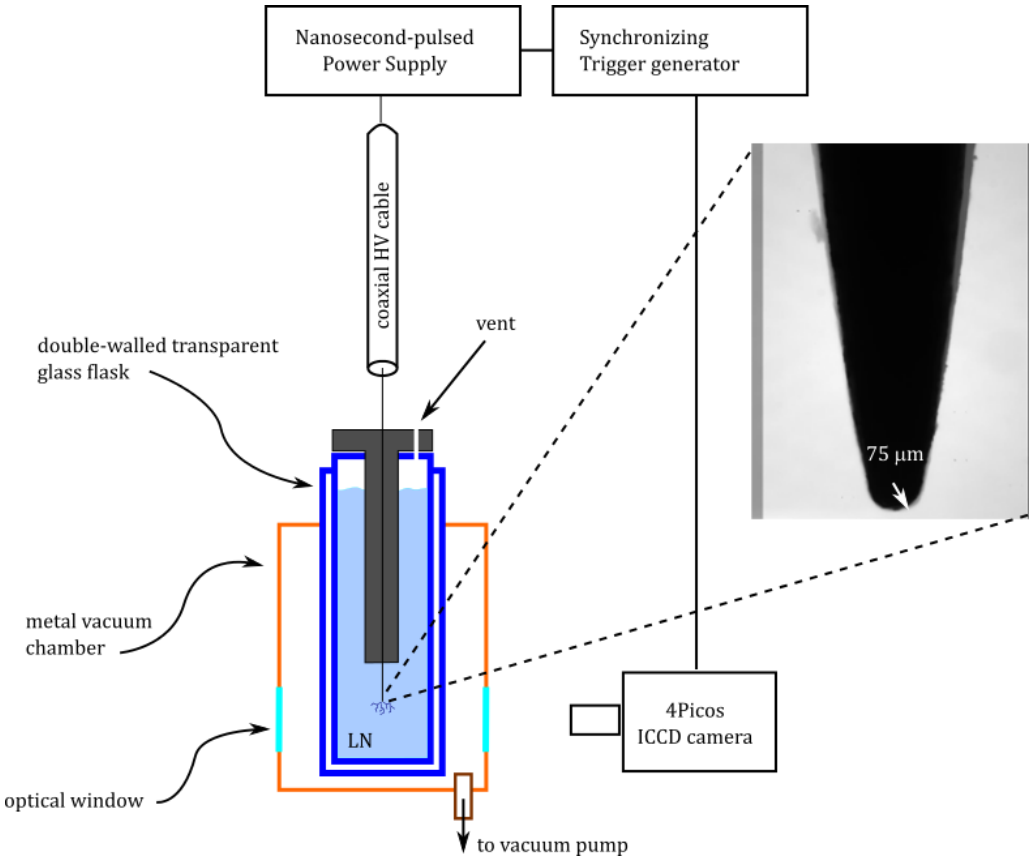

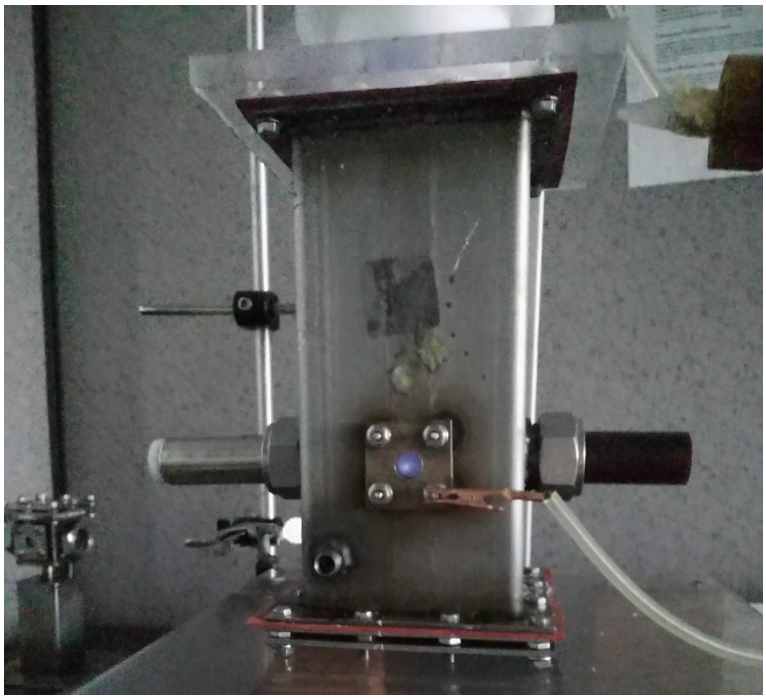

Figure 1. Schematic and photograph of an experimental setup for generation of corona discharge in liquid nitrogen

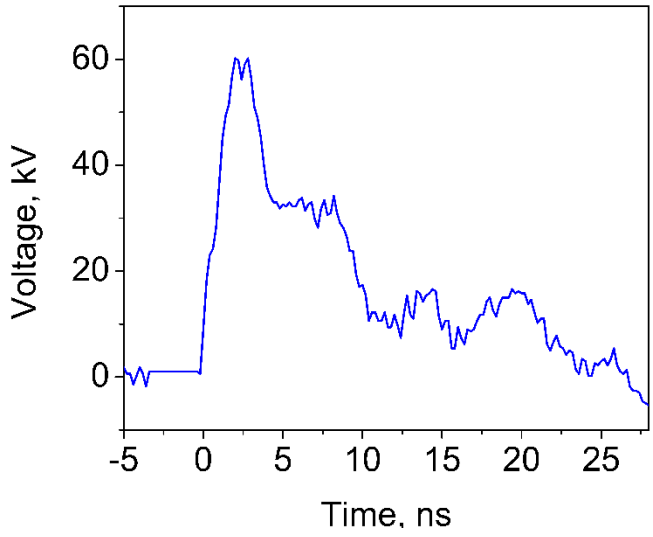

Figure 2. Typical high voltage pulse waveform generated by FPG 120-01NM10 nanosecond-pulsed power supply

For generation of spark discharge in liquid nitrogen, two stainless-steel needles with ~100 μm tip curvature were fixed with ~0.1 mm gap in a plastic (50 ml) chamber covered with lid (Figure 3).

High voltage pulses were generated using 20-01NK high voltage plasma source (FID Tech Company) capable of providing pulses with maximum amplitude of 23.7 kV and duration (63% amplitude) of 12.5 ns. In these experiments spark discharge was ignited with 20 kV amplitude pulses. High voltage pulses were delivered to the electrodes via either 30 or 3 m long $RG\ 393/U$ 50 Ohm high voltage coaxial cable. Pulse shape monitoring and voltage measurements were done using calibrated back current shunt mounted on the long cable and P6015A high-voltage probe (75-MHz bandwidth, Tektronix). Discharge current was measured using current monitor (6585, Pearson Electronics Inc.) connected to a digital phosphor oscilloscope (DPO 4104B, Tektronix).

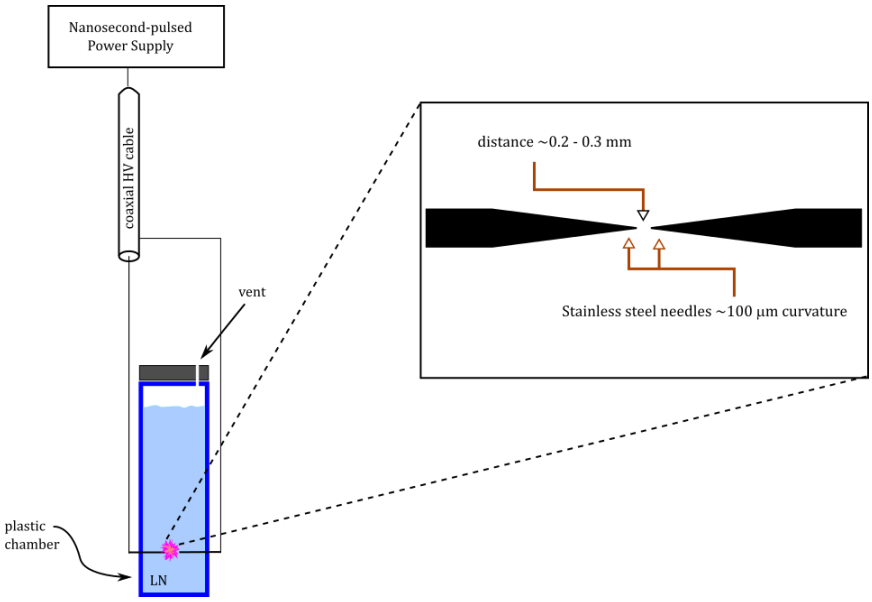

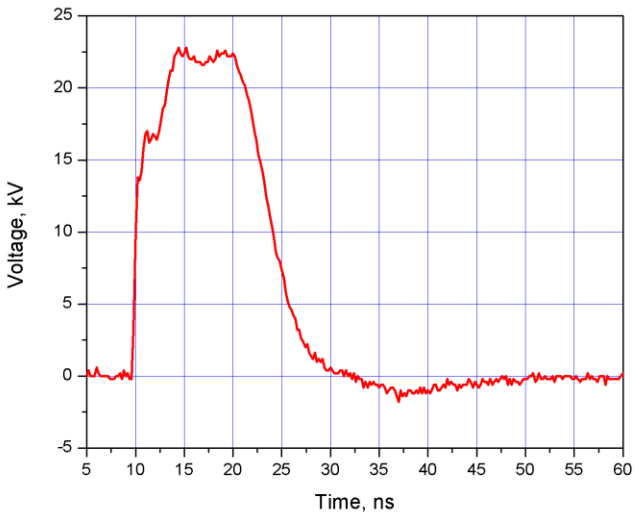

Figure 3. Schematic and an experimental setup for generation of spark discharge in liquid nitrogen and typical HV pulse waveform.

Discharge emission spectrum was obtained using Princeton Instruments-Acton Research TriVista TR555 spectrometer system via 1 m single leg fiber optic bundle with nineteen 200 μm fibers (190 – 1100 nm, Princeton Instruments, USA) and Princeton Instruments PIMAX ICCD camera was used for light registration. The same spectrometer in combination with SDM532-100SM-L 532 nm Spectrum Stabilized Laser Module (Newport) and RPB532 Raman probe (InPhotonics) was used for measurements of Raman spectrum. Raman spectra were registered from the both treated and untreated samples directly in liquid nitrogen with few mm thick liquid layer (in low form Dewar flask, CG-1592-03, Chemglass Life Sciences, USA). Raman spectrum of heated sample was done in room air – treated azide was placed in covered (to avoid water condensation on the sample) glass Petri dish and allowed to warm up to approximately -8 ^{0}C. FTIR measurements were performed using Nicolet 8700 FTIR spectrometer. For measurements of the infrared absorption spectra, treated samples were placed between KBr windows (25x4 mm, Pike Technologies, USA) that were cooled in liquid nitrogen using cooled sample holder (Universal Sample Holder, Thermo Scientific, USA). Measurements were done in nitrogen atmosphere to avoid water condensation on the windows and within a minute after placement of the sample into the measurement compartment of the spectrometer (corresponding temperature increase of the windows and the sample holder was less than ~50 K as measured by thermocouple). X-ray diffraction pattern was collected using Rigaku SmartLab X-Ray diffractometer (CuKα = 1.54 Å); for that, sample holder was cooled in liquid nitrogen and the spectra were collected in several steps to minimize sample heating (a portion of the same treated sample were used).

3. Nanosecond-pulsed plasma generation in liquid nitrogen imaging and temperature measurements

Discharge imaging

Figure 4 shows long (5 ns) exposure images of the discharge in liquid nitrogen take with 5 ns time step. The discharge is visible using ICCD camera for about 30 ns, and high voltage pulse reflections are absorbed by the power supply. This is in contrast to other studies (see, for example, [1-4]) where reflected pulses resulted in successive discharge ignitions in the gaseous voids (bubbles).

Typical discharge size was on the order of few mm and appears to be significantly larger that reported previously for slower but lower voltage (~30 kV) pulses applied for generation of streamer in liquid nitrogen (although in our experiments the electrode size is also quite large compared to 1 μm needle used in [5]). From these images, we estimate streamer propagation velocity to be at least $0.7 \div 0.8 \times 10^3$ km/s (here we used relatively long exposure time of 5 ns). Previously, similar propagation velocities were reported for the discharges in water (see, for

example, [4, 6, 7]), however in [5] and [8] streamer propagation velocities in LN were an order of magnitude lower.

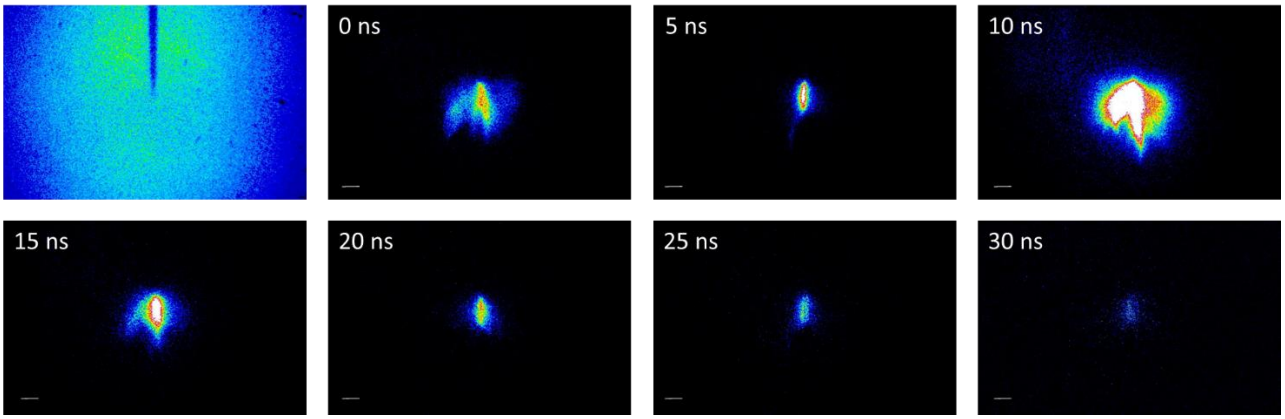

Figure 4. The high voltage needle and long exposure ICCD images (false colored) of the nanosecond-pulsed discharge in liquid nitrogen. Exposure time was 5 ns and time delay between the pulses was 5 ns. The time stamp corresponds to the arrival of the high voltage pulse to the discharge gap. White bar is 1 mm.

In order to examine whether the discharge is ignited in preexisting gaseous bubbles which could be present from, for example, previous discharge ignitions, evaporation of nitrogen on the needle, we have performed shadow imaging of the discharge. The results (Figure 5) indicated that no large-scale irregularities exist in liquid before the discharge, and only after about 15 ns, when the main plasma event starts to decay, visible gas voids start to appear at the location of the streamers. This corresponds well with the observations made previously for the nanosecond discharge in water [2].

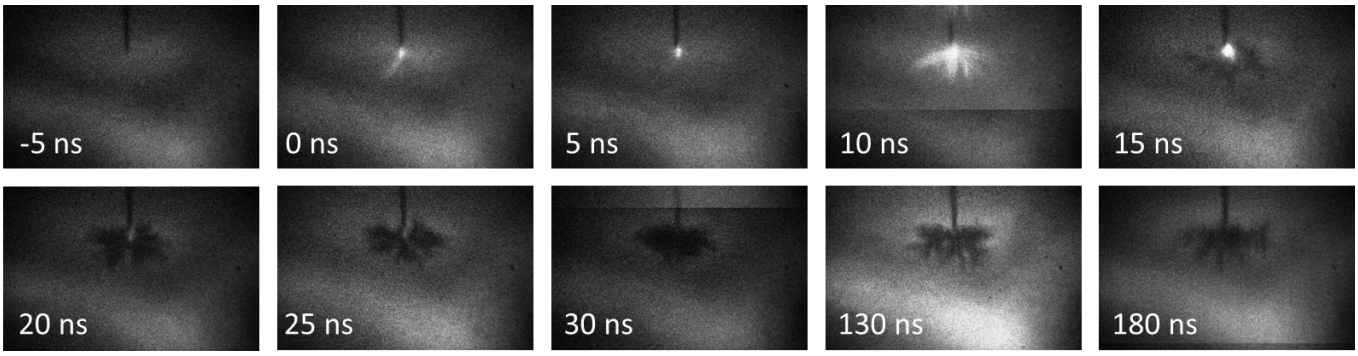

Figure 5. Shadow imaging of the nanosecond-pulsed discharge in liquid nitrogen showing ignition in liquid phase and formation of gaseous voids after the main discharge pulse.

Optical emission spectra of the nanosecond-pulsed discharge in liquid nitrogen

Emission of the discharge in 300 – 415 nm range was recorded using 4Picos ICCD camera with either 100 ns exposure time single accumulation or 3 ns exposure time and 50 accumulations. Obtained spectra are shown in Figure 6, where the short exposure time spectra are shown with the time corrected for the light propagation delay in the optical fiber and spectrometer (compared to the discharge imaging system). It is interesting that the emission spectrum in this range (300 – 415 nm) is mostly from molecular nitrogen emission lines – second positive system $C\ ^3\Pi_u$-$B\ ^3\Pi_g$ (SPS). We also observed the first positive system $B\ ^3\Pi_g$ – $A^3\Sigma_u^+$ emission in 700 – 900 nm range as well as some atomic nitrogen emission lines, but due to high noise the data are not shown here. Using ro-vibrational emission spectrum of the 0-0 $C\ ^3\Pi_u$-$B\ ^3\Pi_g$ transition (SPS) at around 337 nm and assuming equilibrium of the rotational temperature T_r(C) of the C state and T_r(X) of the ground state of nitrogen we have estimated the temperature of the discharge (Figure 6). The rotational temperature of nitrogen was estimated by fitting a synthetic spectrum to the experimental spectrum of the 337 nm transition emission band of the second positive system of nitrogen with the program Specair 3.0 [9] (Figure 6). Simulation of the long exposure (100 ns) spectrum shown in Figure 6 resulted in the estimated temperature value of ~110 K, and the maximum discharge temperature obtained from the time resolved spectra is around 140 K – about 60 K above liquid nitrogen temperature. These data, however, should be further analyzed as it is not clear if the emission originates from the gaseous voids, as well as applicability of this analysis technique for liquid state has not been checked. Previously, spectroscopic measurements of nanosecond-pulsed streamers in liquid nitrogen were done for slower but probably more energetic pulses – estimated temperature was ~500 K [5]. It is important to notice, however, that in our experiments we have not observed significant broadening of the emission lines (in contrast to water experiments) which could in fact indicate that the emission originated from the low-density regions.

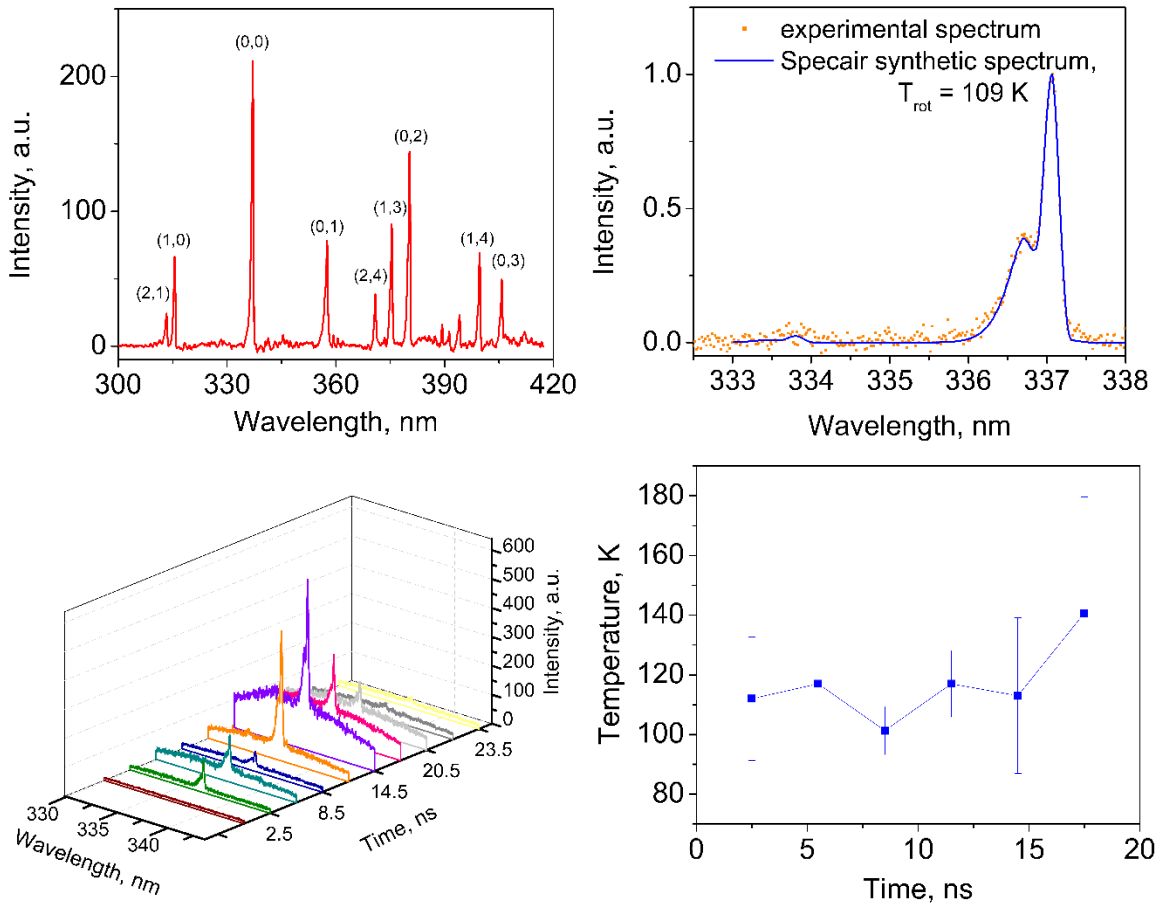

Figure 6. Emission spectra of the nanosecond-pulsed discharge in liquid nitrogen: overview of the 300-415 nm range integral (100 ns exposure time, single accumulation) emission (top left); comparison of experimental and Specair [9] simulated spectral line for 100 ns exposure time (top right); time-resolved 337 nm line emission (3 ns exposure, 50 accumulations, bottom left); and liquid nitrogen rotational temperature evolution as a function of time obtained from Specair [29] simulations (bottom right).

Spark discharge in liquid nitrogen ignition and characterization

Nanosecond-pulsed spark discharge in liquid nitrogen was ignited using both long and short cables to deliver the high voltage pulses from the power supply to the electrodes. The longer cable delivers high voltage pulses to the electrodes with approximately the same shape (rise time and duration) and amplitude as generated by the power supply, and the discharge is ignited several times as the pulses are traveling along the cable due to the mismatch of impedance between the discharge chamber and the cable as well as the cable and the power supply. These pulse reflections are clearly seen on the oscillogram obtained using the back current shunt (Figure 7): the first voltage pulse is the one that travels from the high voltage power supply to the electrode (and results in the discharge ignition), the second one is the reflected one that is traveling from the discharge

gap back to the power supply (hence, no current peak is seen on the current waveform). In this case, the discharge ignites several times, but a portion of the energy is deposited in the cable. Total energy of the discharges ignited within one sequence was ~58 mJ, with the energy of the 1st discharge being ~17 mJ. In contrast, sparks generated using the shorter high voltage cable are ignited as a longer (almost 1 μs long) and hotter plasmas; this is because the duration of the high voltage pulse is longer than it takes it to propagate from the power supply to the discharge gap (it takes ~14 ns for a signal to travel along a 3 m cable). In this case, the entire length of the cable is essentially at the same potential and acts as a capacitive element with capacitance of ~300 pF, which results in characteristic current waveform. Total discharge energy measured was ~43 mJ.

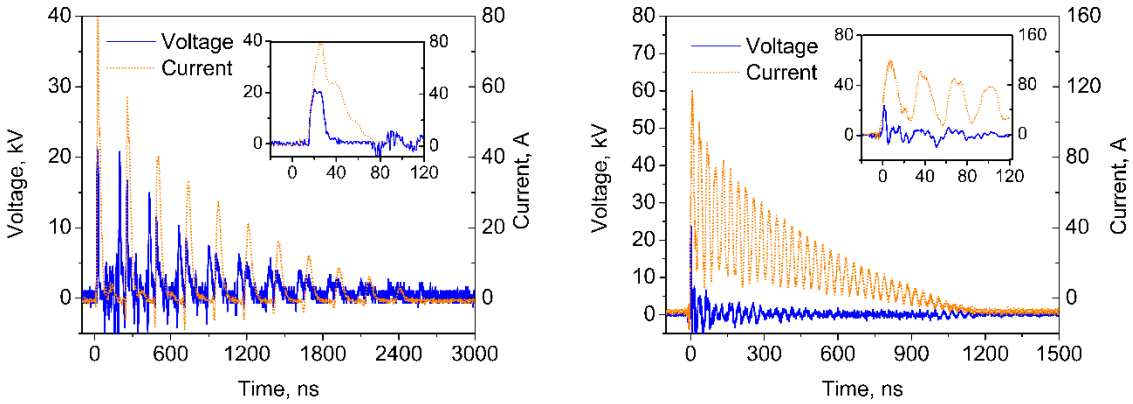

Figure 7. Current and voltage waveforms of spark discharges in liquid nitrogen ignited using 30 m "long" (left) and 3 m "short" (right) high voltage cables for delivery of nanosecond pulses to the electrodes.

Optical emission spectra of the discharges ignited via long and short cables show significant difference (Figure 8). All spectra were obtained using 10 signal accumulations with the discharge running at 30 Hz repetition frequency. In the case of long cable, the spectra of the first discharge ignition (first pulse) recorded with 100 ns exposure time, besides intense broadband background emission, show only lines of atomic nitrogen and nitrogen ion. With longer integration time, 1 s, we were able to record the emission spectrum from the whole discharge, including its multiple reignitions due to the pulse reflections; here we notice appearance of additional metal lines originating from the electrode material. We, therefore, hypothesize that the discharge is ignited inside of a nitrogen bubbles, and successive ignitions result in evaporation of the electrode material resulting in electrode erosion and appearance of metal lines in the spectrum. This is very similar to what was observed previously in nanosecond-pulsed discharge ignited in liquid nitrogen, where the authors observed metal melting after ~100-300 ns after the first discharge initiation. In contrast, spectrum of the discharge ignited using short cable (10 ms integration time) is densely populated with atomic metal lines, which confirms its thermal nature due to much longer discharge duration and, consequently, higher temperatures and concentrations of the melted metal material from the electrodes. In this case, we have also observed significant electrode erosion: after 30 minutes, stainless steel high voltage electrode erosion caused its shortening of ~300 μm with corresponding weight decrease of 0.4 mg; grounded electrode shortened by ~800 μm and ~0.8 mg decrease of weight was observed.

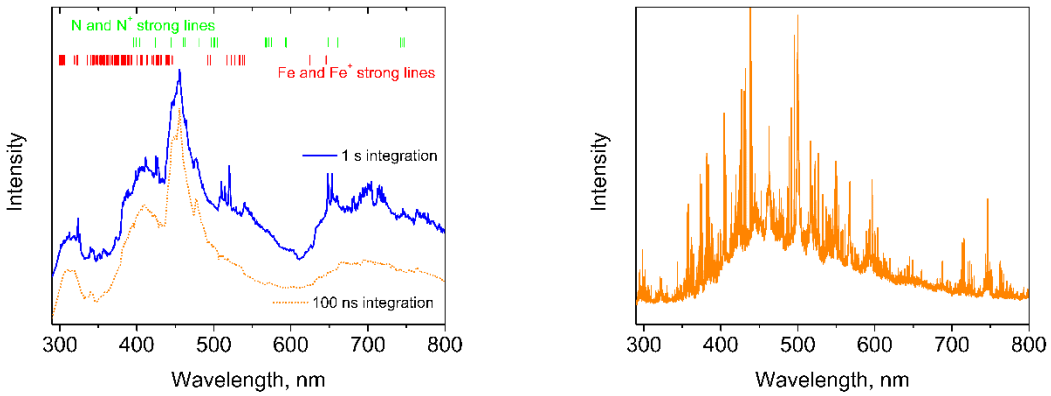

Figure 8. Optical emission spectra of spark discharges in liquid nitrogen ignited using 30 m "long" (left) and 3 m "short" (right) high voltage cables for delivery of nanosecond pulses to the electrodes.

4. Characterization of the plasma-generated materials

Nitrogen material production by the nanosecond-pulsed discharge in liquid nitrogen

Nanosecond-pulsed discharge was used for treatment of the liquid nitrogen. Treatment duration was 30 – 60 minutes at pulse repetition frequency of 60 Hz. After 60 minutes of treatment, no significant erosion of the high voltage electrode was registered (Figure 9). Liquid nitrogen after 1 hour of treatment (about 50 mL) was heated in room air and in He atmosphere (closed vessel) on a hot plate (temperature around 400 °C) in order to increase the concentration of the produced material. With evaporation of the liquid nitrogen the liquid darkened leaving a black powder-like material (see Figure 9), and within a second exploded with generation of both light and sound. No residue was left after the material decomposition. The observed material appears to be very similar to the one described in [10] – a solid amorphous non-molecular form of nitrogen.

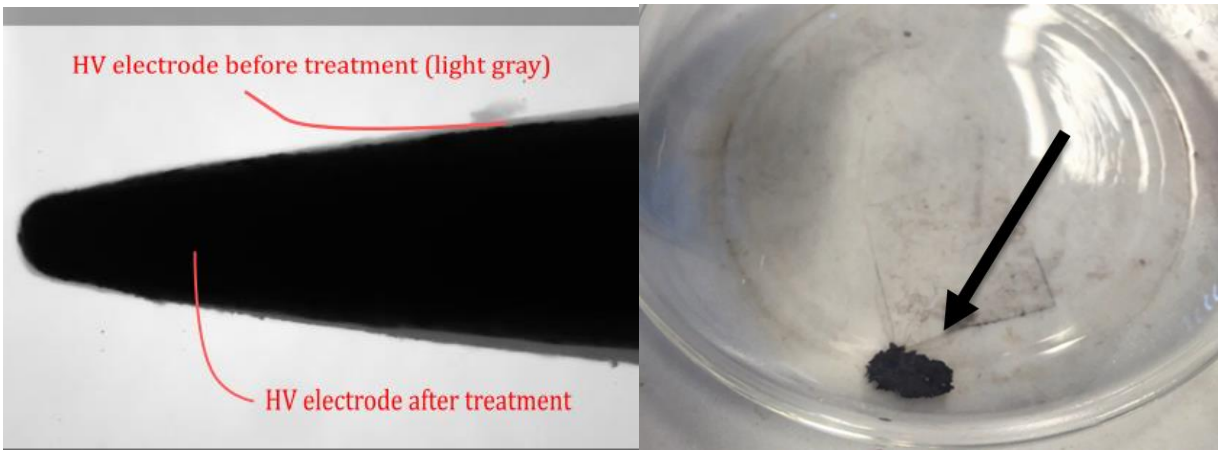

Figure 9. High voltage electrode before and after 1-hour treatment of liquid nitrogen at 60 Hz pulse repetition frequency (left) and black powder material produced as the results of 1 hour treatment and after evaporation of excess liquid nitrogen (right).

We attempted to measure Raman spectrum of the obtained material. Raman spectrum of the liquid nitrogen changes after treatment (Figure 10) but is difficult to interpret. Nitrogen vibron at around 2330 cm^{-1} is present in both treated and untreated samples. Similarly to [10-14], we notice vibron excitation in the vicinity of the main 2330 cm^{-1} peak which could indicate appearance of new phase. Broad features around 800 cm^{-1}, 930 cm^{-1} and 1050 cm^{-1} probably could be assigned to N-N modes (e.g., compared to calculations and measurements from [15] where line at 1060 cm^{-1} corresponds to N_8^- vibrational frequency) likely broadened due to structural disordering (amorphization), however it is difficult to interpret and compare these data with previous studies due to large difference in pressures. We did not register characteristics lines from azide groups (1360 cm^{-1}), nor any Raman peaks associated with ozone which further supports our hypothesis on liquid nitrogen-based plasma production of energetic nonmolecular form of nitrogen-rich material.

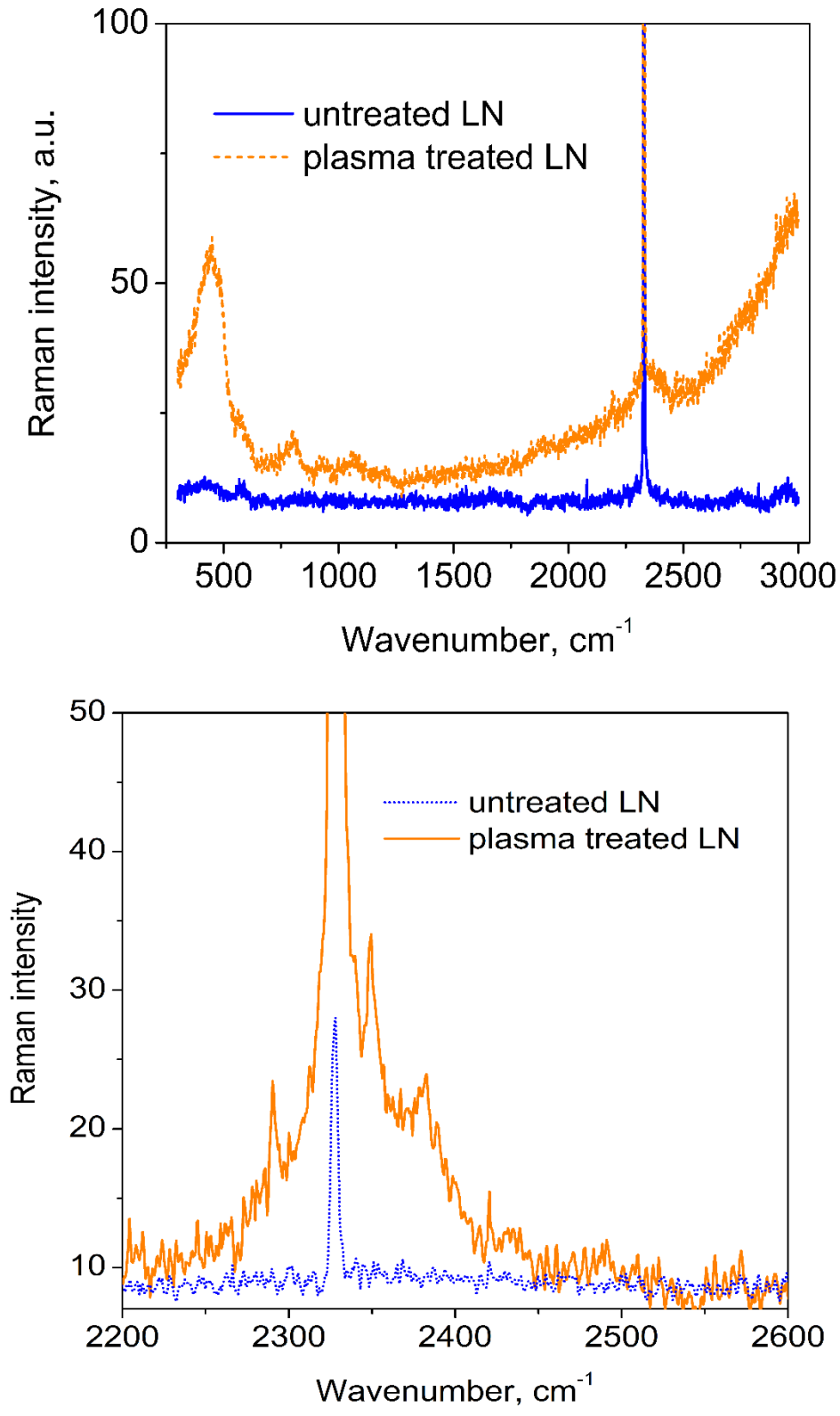

Figure 10. Raman spectrum of the produced material: overview and nitrogen vibrons in the 2300-2400 cm^{-1} range.

FTIR analysis of the gaseous products of sample evaporation and decomposition in air (explosion) was done using Nicolet 8700 FTIR spectrometer equipped with 2 m gas cell. For *evaporation* products measurements, the samples were placed in tightly closed reaction vessel with outlet connected to the spectrometer gas cell; in order to prevent possible reactions with room air oxygen, additional He flow at rate of 1 slpm was supplied into the system. We also examined the reaction products of the sample decomposition in presence of room air. For that, treated sample was placed into a reaction vessel heated using a hotplate, and room air was pumped into the reaction vessel at flow rate of 1 slpm. The representative spectra are shown in Figure 11.

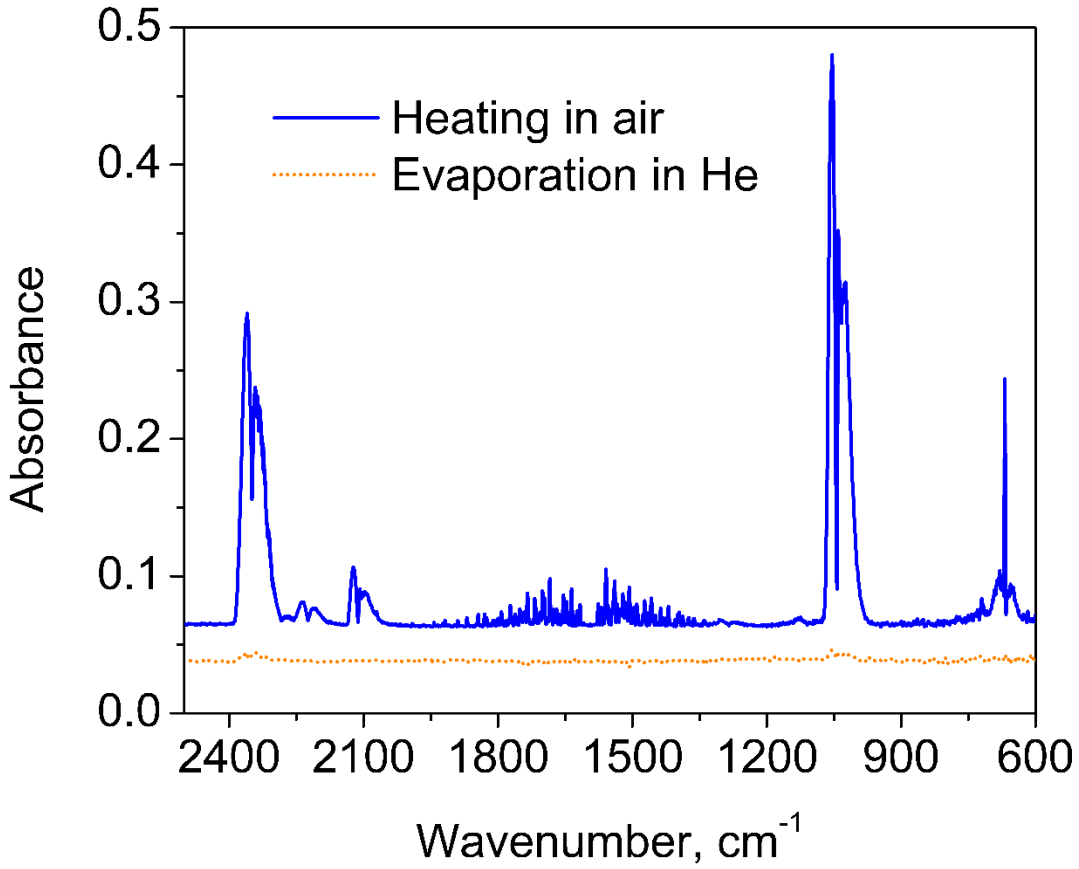

Figure 11. FTIR spectra of gaseous products of the plasma-produced material evaporation in He flow and reaction products of material heating in air flow (spectra are shifted vertically for clarity).

FTIR spectra of the gaseous products from heated samples show peaks of ozone, N_2O, water and CO_2. Samples evaporated in He show significantly lower concentrations of ozone and CO_2. Presence carbon dioxide in evaporated (unheated) sample is due to its presence in liquid nitrogen and contamination from room air. Ozone can be generated in liquid nitrogen during the discharge from the 1% oxygen that is present in the untreated liquid nitrogen, its concentration is relatively low and is estimated to be a few ppm. It is, however, unlikely that presence of ozone and nitrous oxide is the result of their direct generation by the discharge in liquid nitrogen: we have never detected any other NO_x species (e.g., NO, NO_2, N_2O_5) that are traditionally produced in air plasmas

[16]. Moreover, production of atomic nitrogen in presence of molecular oxygen and atomic oxygen in presence of nitrogen immediately leads to generation of NO_x species through, for example [16]:

$$N + O_2 \rightarrow NO + O$$

$$N + O_3 \rightarrow NO + O_2$$

$$O + N(\,^2P) \rightarrow NO^+ + e$$

$$O + NO + M \rightarrow NO_2 + M, M = N_2, O_2, NO, NO_2, N_2O, and\ others$$

In contrast, N_2O can be produced in reaction [16]:

$$N_2(A) + O \rightarrow N_2O + O\ . \tag{1}$$

that does not require availability of NO_x species. This also results in simultaneous production of ozone:

$$\begin{cases} N_2(A) + O_2 \rightarrow N_2(X) + O + O \\ O + O_2 + M \rightarrow O_3 + M \end{cases} \tag{2}$$

During the heating in presence of air, the sample rapidly decomposes with generation of large amount of both ozone and N_2O. In this case, we have registered ozone concentrations up to several percent and N_2O of ~0.1-0.5%. This significant increase of both O_3 and N_2O can be explained by significant energy release during the sample decomposition. Due to absence of NO and other similar species, we hypothesize that one possible mechanism of such rapid production of both nitrous oxide and ozone during the sample decomposition is related to energy release and production of excited nitrogen via reactions (1) and (2). This is somewhat surprising since production of electronically excited nitrogen (triplet sigma nitrogen, $N_2(A^3\Sigma_u^+)$) requires energies on the order of 6.2 eV and it is not typically produced during explosions. On the other hand, the N≡N triple bond energy is characterized by value of 229 kcal/mol (9.9 eV), while the N=N double and N–N single bond energies are only 100 kcal/mol (4.3 eV) and 38 kcal/mol (1.6 eV) respectively. Back conversion to diatomic molecular nitrogen is, therefore, highly exothermic and corresponding energy release could be the source of production of electronically excited $N_2(A^3\Sigma_u^+)$ which leads to generation of N_2O. We cannot definitively claim production of polynitrogen material in our experiments, but multiple N_x all-nitrogen compounds could be formed in the non-thermal plasma in liquid nitrogen. It is easy to imagine, for example, that ions like N_3^+ are produced here which can further polymerize in reactions like $N_3^- + h\nu \rightarrow N_3^{\cdot} + e^-$ *and* $N_3^- + N_3^{\cdot} \rightarrow N_6^-$ [17]. In order to determine exact composition of the produced material, further experimental studies are clearly needed.

5. Nanosecond-pulsed plasma in liquid nitrogen treatment of NaN_3

Treatment of NaN3 in liquid nitrogen using spark discharge

Approximately 1 g of sodium azide (>99%, powder, Fisher Scientific) was added to the liquid nitrogen before treatment. Treatments were done using both higher and lower energy discharge

systems with 200 Hz pulse repetition frequency: we did not observe any significant differences in the appearance and of the treated sodium azide (this indicate that the effects of the electrode erosion and the discharge temperature are probably do not play the major role in the sodium azide transformations), and the results reported below were obtained for the higher energy discharge. After ~5-10 min of treatment, the NaN_3 powder changes color from white to green, and if left in room air treated samples turn yellow as they absorb room water. This initial color change (from white to green) indicates structure changes of the sodium azide following plasma treatment in liquid nitrogen.

We have recorded IR spectrum of both treated and untreated samples (Figure 12). Typical NaN_3 IR lines at around 800, 1630 and 2050 cm^{-1} were detected for the untreated sample. After the plasma treatment, a number of new peaks appear, and peaks at 2350 and 1030 cm^{-1} are especially strong. 2350 cm^{-1} peak (together with much weaker 2281 cm^{-1} and 662 cm^{-1}) probably originate from the solid CO_2 [18] which is present in liquid nitrogen as an impurity. Peak at 1030 cm^{-1} is close to absorption band ν_3 of ozone, however we did not register other vibrational ozone bands at around 1100 and 700 cm^{-1} (ν_1 and ν_2 respectively) [19-22]. We have compared experimental IR absorption spectrum to IR vibrational frequencies of polynitrogen molecules predicted by R. Bartlett and collegues [23]. Strong band at around 1030 cm^{-1} was predicted for a number of polynitrogen molecules, however, combination of the observed lines matches the best N_6 ions (Table 2) [24, 25].

Table 2. List of predicted IR vibrational frequencies of N6 molecules [23] compared to observed lines in this study

Molecule structure	IR frequency calculation, cm^{-1}	Intensity calculation	IR frequency observed, cm^{-1}	Notes
N_6^+ C_{2h} planar ^2B_g	448.2	3.5	447	Weak
	584	12.6	533	weak
	1036	112	1030	Strong
	2191.8	206	2185 2146	Weak Broad
N_6^+ C_{2v} planar ^2B_g	530.7	0.5	533	Weak
	769.1 840.9 844.6	46.4 35 12.8	853	Broad
	1281.6	0.7	1295	Weak
	2138.7	54.1	2146	Broad
	2189.5	35.3	2184	Weak
N_6^- C_s $^2A'$	415.2	4.8	412	
	511.3	5.6	511	Weak
	661.4	109	662	Strong
	882.4	32.9	853	Broad
	1016.3	192.9	1030	Strong
	1283.2	11	1298	Weak
	1636.8	390.5	1599	Broad
	2145.5	936	2146	Broad

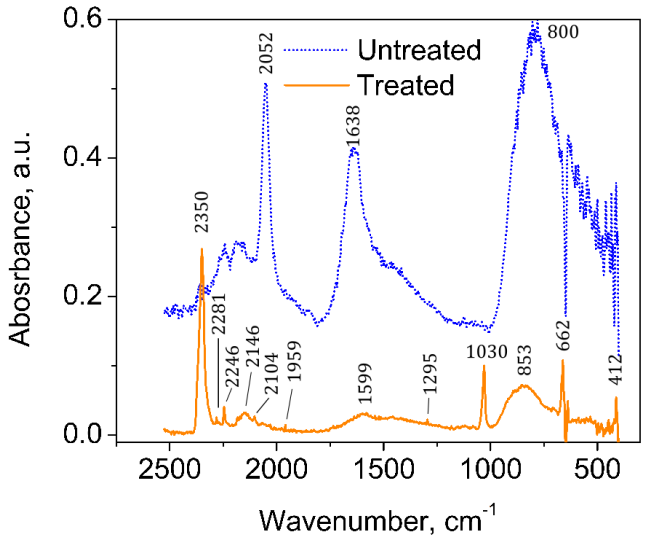

Figure 12. FTIR spectra of untreated NaN3 and NaN3 treated with nanosecond-pulsed spark plasma in liquid nitrogen

Raman spectra of untreated azide, treated azide and treated azide heated to -8 °C show characteristic NaN_3 peaks at 1273 and 1369 cm^{-1} (Figure 13). After treatment, additional peaks appear in the Raman spectrum which is similar to spectrum of azide treated with X-ray and UV at elevated pressures [26]. No Raman peaks of ozone were registered in these experiments. Numerical calculations for Raman vibrational frequencies for N_6^- ions predict strong Raman peaks at around 1283 and 1636 cm^{-1}, as well as other N_6 molecules vibrational bands close to the observed ones (although predicted intensities are low). Following analysis in [27]:

- Peak at ~1660 cm^{-1} can probably be assigned to ν_s(N=N)
- The intensity enhancement of the ν_b(N3) modes at around 610 cm^{-1} (at higher pressures in cited study – 640 cm^{-1}) could indicate the change in linear N=N=N to bent N=N-N.

We have followed the peak at 1660 cm^{-1} as a function of temperature of treated azide. The result (compared to relatively constant intensity of 1369 cm^{-1} peak) show disappearance of the 1660 cm^{-1} peak at around -55^{0}C, which could indicate that the obtained material is stable up to this temperature at ambient pressure conditions.

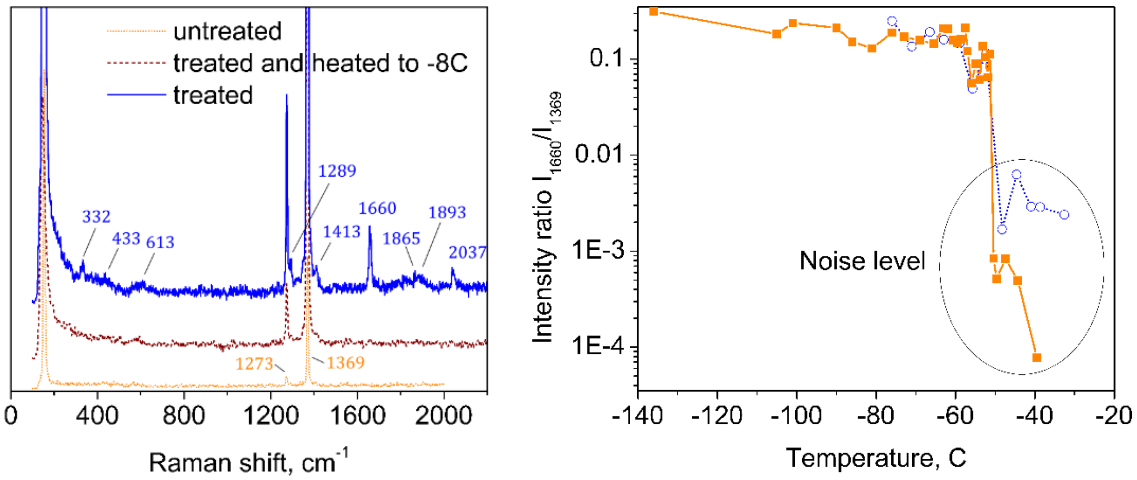

Figure 13. Raman spectra of NaN_3 treated with spark discharge in liquid nitrogen compared to untreated material (left); change of intensity ratio of new 1660 cm^{-1} peak to 1369 cm^{-1} azide peak with temperature increase of the treated sample (two separate experiments shown)

X-ray diffraction pattern (Figure 14) here is compared to XRD data from [28] obtained using the same λ ~ 1.54 Å (and compared to that for λ = 0.41686 Å employed by Eremets et al. [29]). The lines indicated by steriks at 37, 66 and 77 2θ degrees correspond closely to the (110), (211) and (220) reflections of the cubic gauche structure of polymeric nitrogen reported by Eremets and co-workers. The strong lines correspond to unreacted NaN_3. Our results also show peaks at 38 (new compared to untreated), 68 (new or shifted 0.5 degree compared to untreated) and 76 2θ degrees. In addition, peak at 41.3^0 splits into two new peaks at 40.9^0 and 41.7^0; new peak appears at 73.4^0; peaks at 37.1, 68.7, 78.8 appear shifted to negatively by ~0.5^0 to 36.9, 68.2 and 78.2 correspondingly; peaks at 50.1, 56.6, 60, 63.9, 74.7 and 81.8 are positively shifted to 50.3, 57, 60.2, 64.6, 75.1 and 85.3^0.

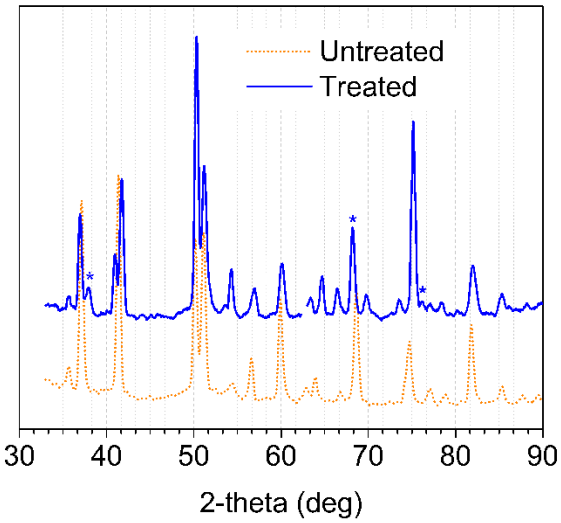

Figure 14. X-ray diffraction spectra of liquid nitrogen spark plasma treated and untreated NaN_3

6. Stabilization of plasma-produced polynitrogen materials

Polynitrogen compounds are linked with nitrogen single bonds. The formation from nitrogen single bonds to nitrogen triple bonds is energy favored based on the exothermic property. Therefore, to change the nitrogen single bonds into other stronger covalent bonds is a possible way to stabilize polynitrogen compounds. Among the possible covalent candidates, the carbon-nitrogen single bonds draw more attention. Carbon-nitrogen bond is one of the most abundant bonds in organic chemistry and biochemistry, it is strongly polarized towards nitrogen and has high dipole moment. The bond length of carbon-nitrogen bond is slightly shorter than carbon single bond in diamond. The stability of cubic gauche carbon nitride (cg-CN) has been evaluated by stimulation and calculation. From the point of view of thermodynamic stabilities, mechanical stabilities, and dynamical stabilities, cg-CN is the most stable among all carbon nitride structures. No experimental work has been done so far on this prediction.

The stabilization of polynitrogen compounds by forming coordination complex is also possible. Many chain or branch-type polynitrogen compounds are calculated to be lower in energy than their cyclic or polycyclic isomers. Homoleptic polynitrogen rings may be the first to focus on because of lack of synthetic paths. The overall strength of a chain or cycled molecule depends on the weakest link on it. In order to stabilize nitrogen cycles it is important to devoid any isolated nitrogen single bond that cannot gain partial multiple bond character through resonance with neighboring bonds. The initial candidate was achieved in 1999 by synthesis of $N5^+$ ion in the form of a marginally stable $AsF6^-$ salt. [31]

Planar nitrogen systems such as cyclo-$N5^-$ and $N5^+$ tend to be more stable than nonplanar systems such as the neutral cyclo-N6. In cyclo-N5 systems a six-π-electron system is created upon either adding to or removing from the cyclo-N5 radical one electron. Separating σ and π electron systems is also a way to stabilizing polynitrogen compounds [32]. The separation of σ and π electron systems can be accomplished by adding oxygen atoms to polynitrogen ring compounds such as cyclo-N4 and cyclo-N6. The addition can increase their thermodynamic and kinetic stabilities, accompanied by only a small reduction in their efficiency as high energy density materials. Coordination of one or more oxygen atoms to the ring leads to effective separation of the σ and π electron systems helping to stabilize the systems.

In our experiments we have explored several ways to stabilize plasma-produced polynitrogen materials:

1) Earlier calculations indicate that surfaces may play an important role in the stability of the cg-N crystal. Potential applications of this material may therefore be limited by the unstable character of its surfaces. Comparative research has been done and the presence of H atoms on the surface helps some surfaces to become more stable. More information is needed on this candidate [33].

   Researchers proposed carbon nanotube as a good agent to stabilize polynitrogen compounds based on its confining and stabilizing function for metastable N8 polymeric

nitrogen clusters [34]. However, for our plasma conditions, it has been proved that a carbon nanotube substrate is not a requirement for cg-N formation [35].

Another carbon compound called C60 is also a possible way for stabilization of polynitrogen compounds [36]. The polynitrogen compounds formed inside C60 are found to be quite stable in confinement. The maximum number of nitrogen atoms that can be encapsulated inside C60 is 13, which can form stable structure at 0K. The endohedral molecules Nn@C60 for $n \leq 12$, are found to retain their structure at room temperature. This suggests the strong possibility of synthesizing polynitrogen compounds in confinement which could be triggered with suitable combinations of oxygen and hydrogen for extracting tremendous amount of energy. The amount of energy density from conversion of lower order bonds to triple bonds comes out to be about three times in contrast to the conventional chemical energetic materials.

In our experiments, we have used two forms of carbon material: activated carbon and Boron nitride nanotubes (Sigma Aldrich, Multiwalled, powder, >25%).

In the first set of experiments, we have used manually crushed activated carbon (powdered) and added into treated for 2 hours using nanosecond-pulsed spark liquid nitrogen. The solution was then left for reaction overnight (~18 hours). The product was then examined using Raman setup; spectra were taken with liquid nitrogen present and right after it evaporated. The results (Figure 15) show appearance of a new strong peak at ~1660 cm^{-1} which was previously observed in experiments with plasma-treated NaN3. Numerical calculations [8] for Raman vibrational frequencies for N_6^- ions predict strong Raman peaks at around 1283 and 1636 cm^{-1}, as well as other N_6 molecules vibrational bands close to the observed ones (although predicted intensities are low):

- Peak at ~1660 cm^{-1} can probably be assigned to ν_s(N=N)
- In contrast to plasma-treated NaN3, here we did not observe any new peaks near 1283 cm^{-1}.
- The intensity enhancement of the ν_b(N3) modes at around 610 cm^{-1} (at higher pressures in cited study – 640 cm^{-1}) could indicate the change in linear N=N=N to bent N=N-N.
- Predicted peaks near 392, 415 and 882 cm^{-1} were observed at 390, 433 and 917 cm^{-1} respectively.

After liquid nitrogen evaporation, however, these new peaks have disappeared.

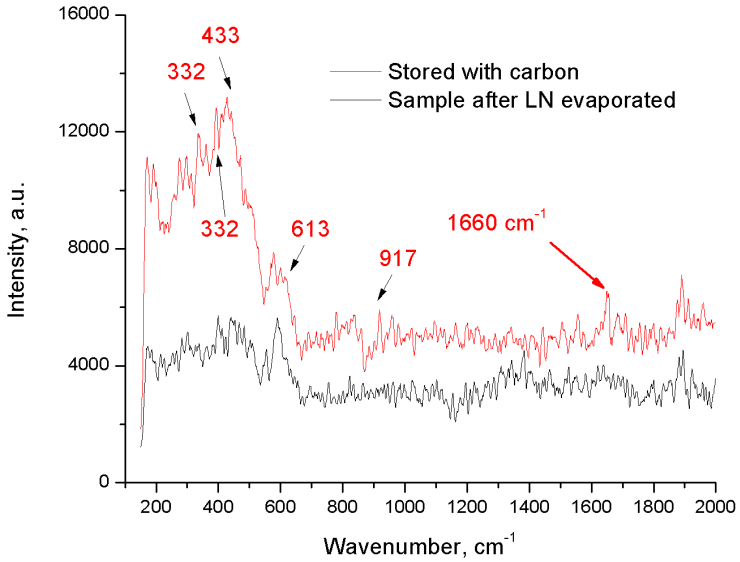

Figure 15. Raman spectra of plasma-treated liquid nitrogen stored with activated carbon overnight: before and after evaporation of liquid nitrogen.

Plasma treatment of liquid nitrogen was also done in presence of Boron nitride nanotubes using spark plasma. The Raman spectra show appearance of new peaks around 1580 and 2310 cm^{-1} which then disappeared after evaporation of LN (Figure 16):

- several polynitrogen molecules predicted [23] to have Raman active vibrational frequencies around 1580 cm^{-1}: N_3^+ at 1549 cm^{-1}; N_5^+ D_{2d} at 1569 cm^{-1} (predicted weak peak at 674 cm^{-1} not observed); N_6 C_2 book at 1575 cm^{-1} (predicted weak peaks at 812 and 1012 cm^{-1} not observed), several N_8 at around 1550-1570 cm^{-1}.
- Strong peaks at 2294 and 2349 with relative intensities of 23 and 188 (with other significantly weaker peaks) were predicted for N_5^+ C_{2v} [23].

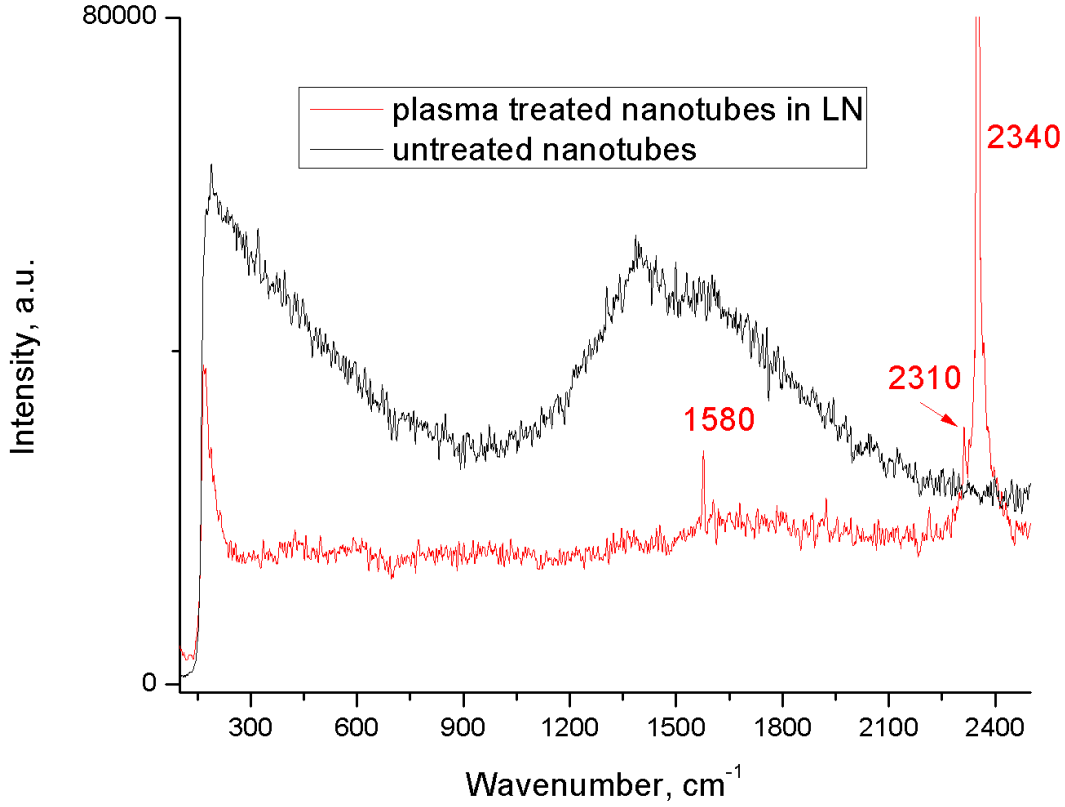

Figure 16. Raman spectra of plasma-treated liquid nitrogen with Boron nitride nanotubes.

2) The only bulk stable neutral energetic polynitrogen compound, cubic-gauche polymeric nitrogen (cg-N), was synthesized under pressure, at 110GPa. In that same pressure regime, other polynitrogen anions were discovered, such as infinite 1D armchair chains (in FeN4 and ReN8·xN2) and the pentazolate ring (N5−), found in CsN5. Mg-N bonds are also be found to be relatively stable under ambient pressure. Among them, the compression of magnesium and nitrogen was predicted to produce the MgN3, MgN4, and MgN10 salts comprised of exotic anionic benzene-like N6 rings, infinite 1D armchair chains and pentazolates, respectively. Magnesium (Sigma, powder, −325 mesh, 99.5% trace metals basis) was added directly into our systems (both corona and spark plasmas) and treated for 15 minutes.

   Raman spectra of both corona- and spark-treated Mg powder (Figure 17) show similar new peaks that disappear after LN evaporation: broad 430, 520 and 615 cm^{-1} and strong 1580, 1650 (1660) and 2310 cm^{-1}. Similar to experiments with nanotubes and NaN_3, we attribute these new peaks to either N_6 or N_5 molecules [23].

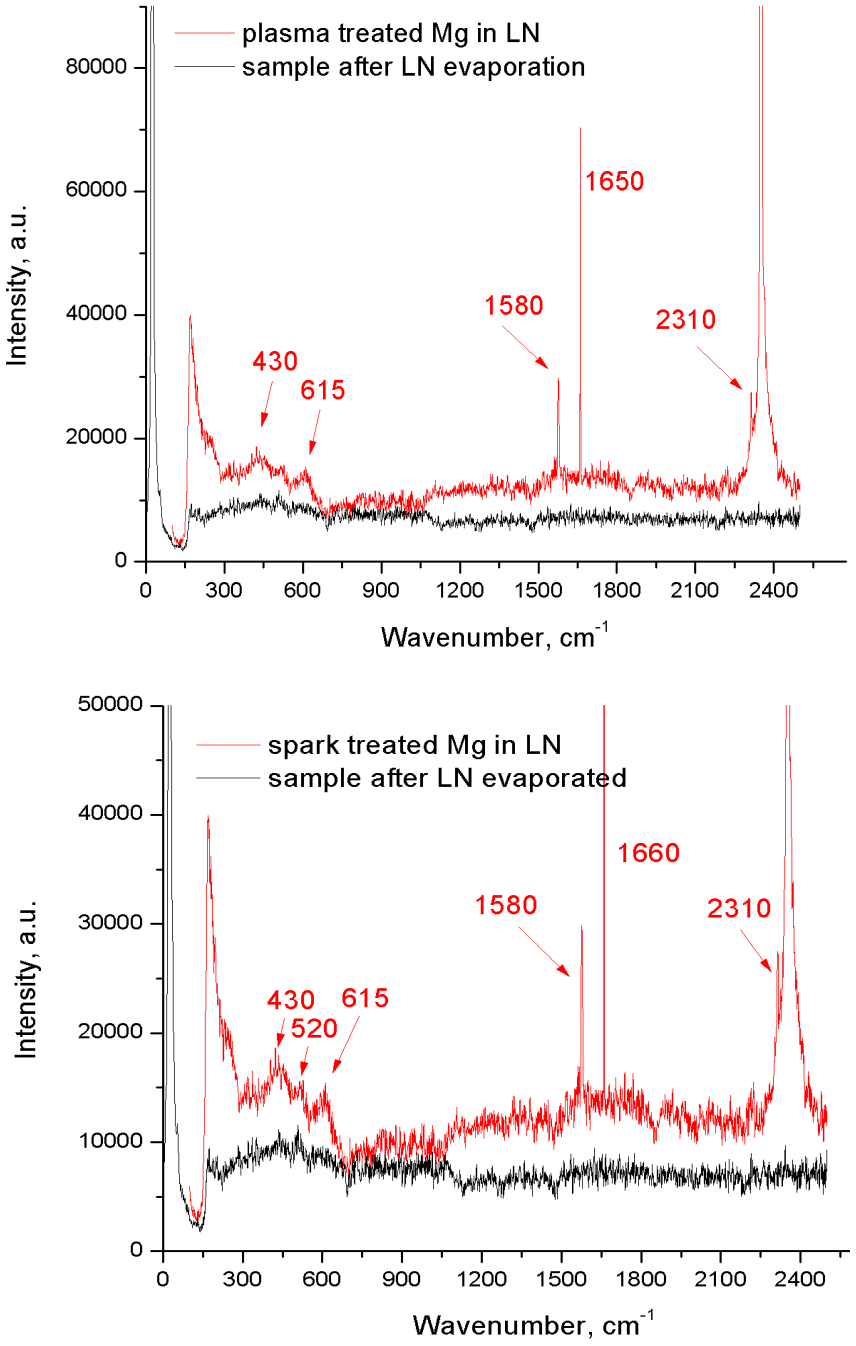

Figure 17. Raman spectra of magnesium powder in liquid nitrogen treated using corona (top) and spark (bottom) plasmas.

3) It is possible to synthesize LiN5 by compressing solid LiN3 and N2 gas under high pressure and quench recover the product to ambient conditions. It is the first time that stable N5− anions are predicted in crystalline states. The weight ratio of nitrogen in LiN5 is nearly 91%, placing LiN5 as a promising high-energy material [37].

As the lightest element in alkali metal, lithium can form different nitrides with nitrogen including Li3N, Li2N2, and LiN3, which had been synthesized successfully. Particularly, Lithium-to-nitrogen (Li-N) ratio equals one in Li2N2 which is neither Li-rich compound nor N-rich compound [38].

In our experiments, we have used Lithium amide powder (Sigma, LiNH2, powder, 95%), and treated using both plasma setups for various times. Raman spectra did not show any new peaks.

4) Incorporation of the produced material into porous media – this pathway was suggested earlier. For this, we have used several materials (ceramic with various porosity, zeolite, aluminosilicate and mesoporous aluminum oxide. These materials were treated with plasmas in LN for various times, however Raman spectra did not reveal appearance of new peaks.

5) Nanosecond-pulsed plasma in liquid nitrogen treatment of NaN_3 – stability study

As in our previous experiments, approximately 1 g of sodium azide (>99%, powder, Fisher Scientific) was treated using spark plasma. After ~5-10 min of treatment, the NaN_3 powder changes color from white to green, and if left in room air treated samples turn yellow as they absorb room water. This initial color change (from white to green) indicates structure changes of the sodium azide following plasma treatment in liquid nitrogen.

Raman spectra of untreated and treated azide show characteristic NaN_3 peaks at 1273 and 1369 cm^{-1} (Figure 18) with a number of new peaks. Previously, we have followed the peak at 1660 cm^{-1} as a function of temperature of treated azide. The result (compared to relatively constant intensity of 1369 cm^{-1} peak) show disappearance of the 1660 cm^{-1} peak at around -55^{0}C, which could indicate that the obtained material is stable up to this temperature at ambient pressure conditions.

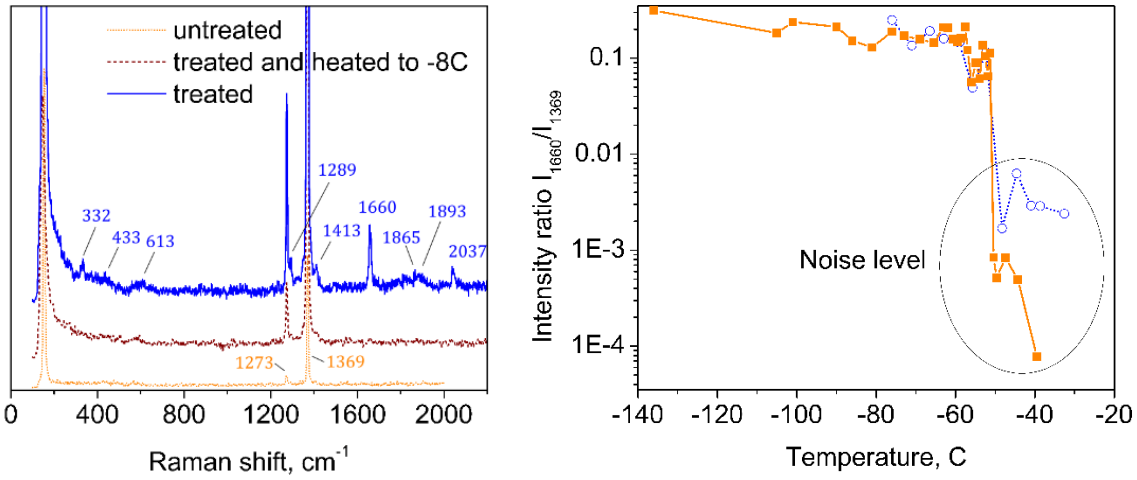

Figure 18. Raman spectra of NaN_3 treated with spark discharge in liquid nitrogen compared to untreated material (left); change of intensity ratio of new 1660 cm^{-1} peak to 1369 cm^{-1} azide peak with temperature increase of the treated sample (two separate experiments shown)

In our new experiments, we have examined stability of the new material at conditions of dry ice (solid CO2) which has temperature of 194.65 K (−78.5 °C). In these experiments, NaN3 was treated using spark plasma for 15 minutes and then placed on a block of solid CO2. Raman spectra, in this case, has shown that the previous observed peak at ~1660 cm^{-1} is actually two peaks at 1665 and 1669 cm-1 (Figure 19). Also, with liquid nitrogen evaporated, a weak peak at around 2342 cm^{-1} (the same position as molecular nitrogen vibron) is still registered.

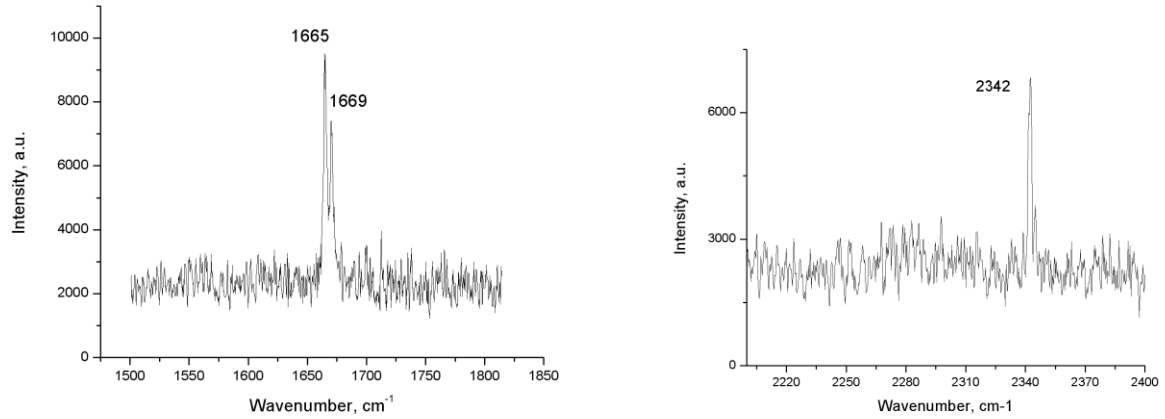

Figure 19. Raman spectra of NaN_3 treated with spark discharge in liquid nitrogen showing douplet line at around 1660 cm^{-1} and weak nitrogen vibron at around 2342 cm^{-1}.

We have followed these peaks (together with azide peak at 1380 cm^{-1}) with time – while the sample was positioned on the block of solid CO2. The results (Figure 20) show that the material lineraly decomposing with time – both 1665 and 2342 cm^{-1} peaks completely disappear within 30 minutes, while the azide peak stays relatively stable. It is possible, however, that the decomposition is related to relatively slow reactions with surrounding air (oxygen and water vapors), therefore we will check the stability in conditions of dry noble gas (Ar or He) atmosphere.

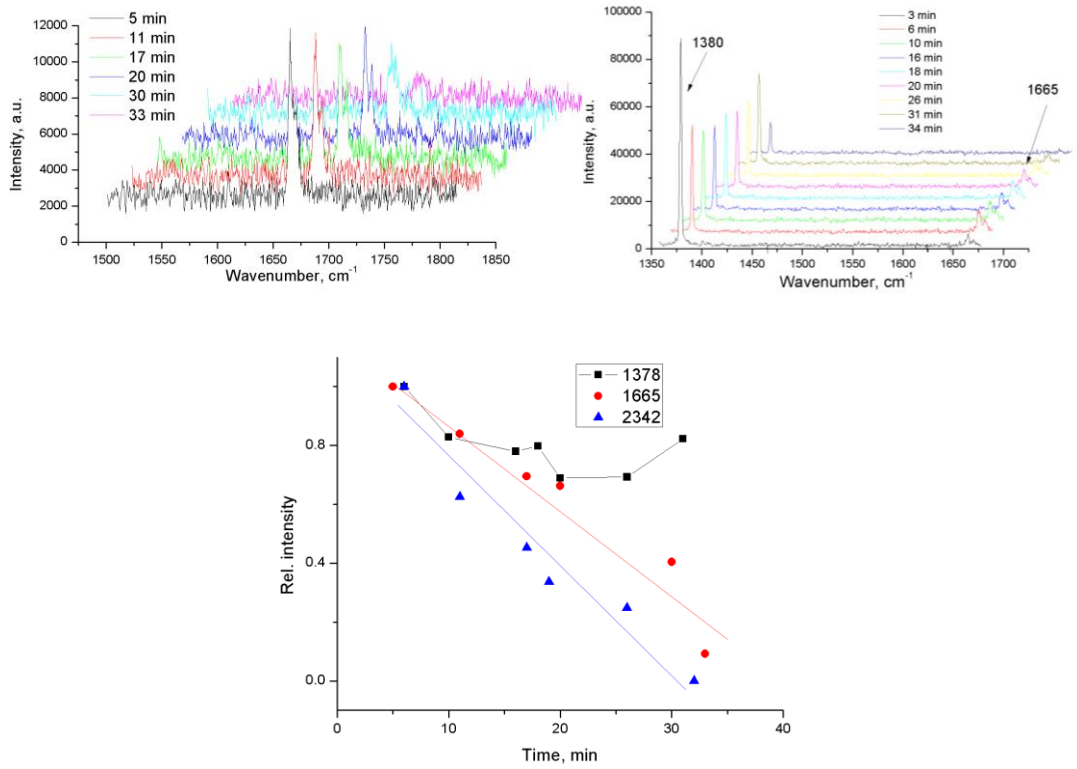

Figure 20. Evolution of the Raman peak intensities of plasma treated NaN3 on solid CO2. Bottom plot shows decrease of normalized intensities with time.

7. Stabilization of plasma-produced polynitrogen materials using adsorbents

We report on experimental study of nanosecond-pulsed plasma treatment of liquid nitrogen demonstrating synthesis of a highly energetic nitrogen material. Raman, FTIR analysis of gas phase products of decomposition, and the material explosion characteristics suggest synthesis of polymeric (amorphous) nitrogen compound which is stable at ambient pressure up to temperatures of about -150 C. Addition of adsorbents with relatively large characteristic pore sizes (>5 nm) allows marginally improved recovery of the material as determined by temperature-dependent Raman measurements. By analyzing the shock wave propagation resulting from the explosions, we estimated the energy density of the material to be 13.3±3.5 kJ/g, close to previously predicted value for amorphous polymeric nitrogen.

For generation of spark discharge in liquid nitrogen, two stainless-steel needles with ~100 μm tip curvature were fixed with ~1 mm gap in a double-walled glass (560 ml) chamber covered with

vented lid. High voltage pulses were generated using FPG 20-1NM10DD high voltage plasma source (FID Tech Company, Germany) capable of providing pulses with maximum amplitude of 26.8 kV, rise time (10-90% amplitude) of 3-4 ns and duration (63% amplitude) of 11.6 ns. High voltage pulses were delivered to the electrodes via 3 m long $RG\ 393/U$ 50 Ohm high voltage coaxial cable.

Industrial grade (99,999% N_2, $O_2 \leq 5$ ppm, $CO_2 \leq 10$ ppm) liquid nitrogen in all experiments was purchased from Airgas, USA. In the Table 3 a list of adsorbents used in the study and their characteristics are presented. In the experiments, the adsorbent materials (50 mg) were added to the liquid nitrogen either before or after the plasma treatment. In all cases, treatment was done using 20 kV amplitude pulses at 1 kHz for 30 minutes.

Table 3. Adsorbents used in the study and their characteristics.

Adsorbent	**Pore size , nm**	**Particle size, μm**
Zeolite (Sigma-Aldrich)	0.1 – 1	< 20
Aluminum oxide, mesoporous (Sigma-Aldrich)	3.8	5.65 μm
Aluminosilicate, mesostructured (Sigma-Aldrich)	2 – 4	-
AmberSep OPTIPORE L-493 (Supelco)	4.6	300 – 800
Diaion HP-2MG methacrylic ester copolymer (Supelco)	17	300 – 750
Diaion HP-20 (Supelco)	26	250 – 850
Crushed granulated activated carbon	>50	-

Sample explosion shadow imaging was done using Miro M310 (Phantom, USA) high-speed camera (15 – 30 μs exposure time; frame rates of 15,000 – 20,000 fps; final image resolution 256×256) and 30 W 1 mm Deuterium arc lamp (Newport, USA) as a source of back light. Sample weight measurements were done using Fisher Scientific Accu-64 analytical balance (readability 0.1 mg).

In this study, we have used a nanosecond-pulsed spark discharge plasma for treatment of liquid nitrogen. Here, we have used a relatively short coaxial high voltage cable which acts as a capacitive element (~300 pF capacitance); this results in continuous reignition of hot nanosecond sparks during the characteristic pulse with total deposited energy of ~36 mJ per event. The pulses were supplied to the discharge chamber at frequency of 1 kHz for 30 minutes, resulting in total energy deposition of ~65 kJ. It must be mentioned that the thermal nature of the discharge results in a noticeable electrode erosion: after 30 minutes of treatment, positive high voltage electrode loose about 0.2 mg, while grounded needle weight reduces by ~1.2 mg.

During the treatment, continuous generation of black microparticles that typically deposit on the bottom of the glass chamber was observed. Upon rapid evaporation of the liquid, these particles

condense leaving an explosive (if heated) black mass; however, explosion happens inconsistently and with various degree of intensity. We have made numerous attempts to obtain a Raman spectrum of the material generated in liquid nitrogen by the plasma – see Figure 21 (a), - and in contrast to our previous study where liquid nitrogen was treated by non-thermal corona-type of plasma, no obvious new peaks were recorded. Instead, the sample typically exhibit strong fluorescence signal from the plasma-generated microparticles, which disappears at around -150 °C (see insert in Figure 21 (a)). Similar Raman spectra (sample fluorescence) was reported previously for high-pressure produced amorphous polynitrogen [39].

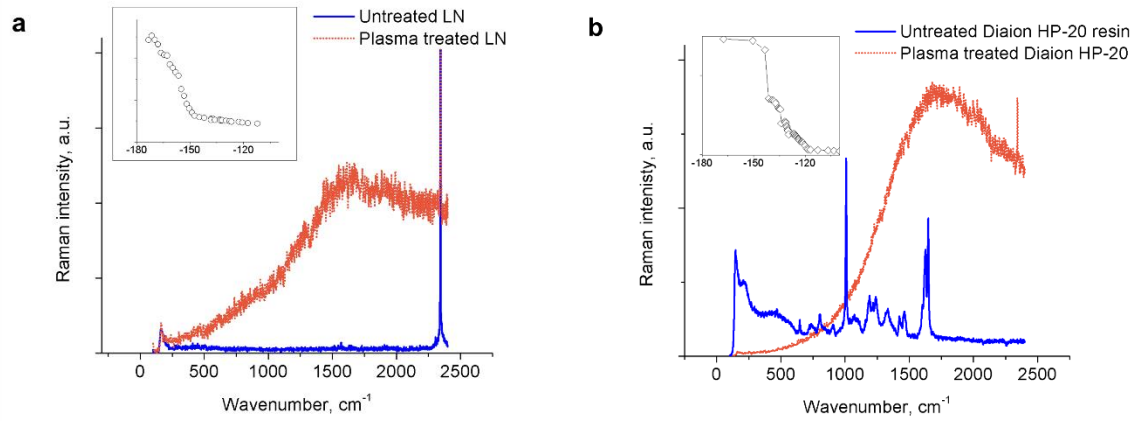

Figure 21. Raman spectra of untreated liquid nitrogen (LN) (a) and Diaion HP-20 resin (b) and treated with nanosecond-pulsed spark plasma. Inserts show decrease of the overall fluorescence intensity with increase of the sample temperature after evaporation of liquid nitrogen (linear scales). Peak around 2330 cm^{-1} originates from molecular nitrogen.

In an attempt to stabilize the plasma-produced material, we have performed a series of experiments in which various adsorbents (50 mg) were introduced either before or after the treatment. Right after the treatment, - or after 1-24 hours of incubation in the experiments when the adsorbent was added after the treatment, - we monitored the explosivity of the samples upon rapid heating. Only the samples that contained adsorbents with larger average pore size - Diaion HP-2MG, Diaion HP-20 and activated carbon, - have exploded. Treatment (or incubation) of the adsorbent resins has also resulted in their color change from white to dark (black). Raman spectra of the treated Diaion HP-20 resin are shown in Figure 21 (b); as in the case of pure liquid nitrogen treatment, we did not register any new Raman peaks, but strong fluorescence which starts to diminish at temperature around -150 °C and disappears at around -120 °C (see insert in Figure 21 (b)). This could indicate marginally improved stability of the physisorbed material. We failed to obtain Raman spectra from the treated activated carbon – visible fluorescent particles escape and their fluorescence fades away (with flashes) under the laser beam, which indicates highly unstable nature of the adsorbed material.

FTIR analysis of the gaseous products of samples treated in presence of adsorbents evaporation and explosion in air was done using Nicolet 8700 FTIR spectrometer equipped with 2 m gas cell. The samples were placed in metal dish open to room air and the reaction products were collected

into the gas cell via a gas flow created by a vacuum pump connected to the outlet of the cell (flow rate ~4 slpm). The representative spectra are shown in Figure 22.

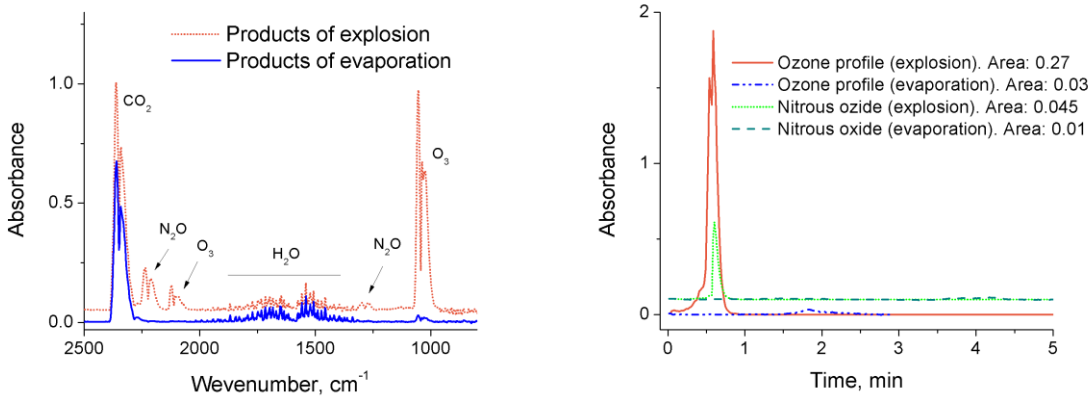

Figure 22. FTIR spectra of gaseous products of the plasma-produced material (treated with activated carbon) evaporation and explosion in air; time evolution of the ozone (1050 cm^{-1}) and nitrous oxide (2235 cm^{-1}) peaks.

FTIR spectra of the gaseous products from all samples indicate presence of ozone, nitrous oxide, water, and carbon dioxide. Evaporated samples show significantly lower concentrations of O_3 and CO_2: carbon dioxide is due to its presence in liquid nitrogen and contamination from room air, while ozone and nitrous oxide can be generated in liquid nitrogen from the oxygen impurities that is present in the untreated liquid nitrogen and contamination during the treatment container filling. It is, however, unlikely that ozone and nitrous oxide are generated directly by the discharge in liquid nitrogen: no other NO_x species have been detected (e.g., NO, NO_2, N_2O_5) while they are usually produced in air plasmas in higher concentrations than nitrous dioxide [16]. Similar effect was noticed in the case of corona-treated liquid nitrogen. As shown in [16], N_2O can be produced in reaction $N_2(A) + O \rightarrow N_2O + O$ that does not require availability of NO_x species. This also results in simultaneous production of ozone:

$$\begin{cases} N_2(A) + O_2 \rightarrow N_2(X) + O + O \\ O + O_2 + M \rightarrow O_3 + M \end{cases}$$

As seen in ozone and nitrous oxide adsorption time profiles (Figure 22), during the explosion of samples in presence of air, large amounts of both ozone and N_2O are being generated. Total area of these profiles indicate that concentrations of these species is almost 5-10 times greater than in the case of evaporation without explosion. We attribute this effect to significant energy release during the sample decomposition: N≡N triple bond energy is characterized by value of 229 kcal/mol (9.9 eV), while the N=N double and N–N single bond energies are only 100 kcal/mol (4.3 eV) and 38 kcal/mol (1.6 eV) respectively. Highly exothermic conversion of single-bonded nitrogen to diatomic molecular nitrogen could be the source of production of electronically excited $N_2(A^3\Sigma_u^+)$ with the energy of 6.2 eV which leads to generation of N_2O. We also hypothesize that registered presence of nitrous oxide and ozone is related to the same processes due to decomposition of material produced by plasma inside of the treatment chamber (because of, for example, plasma-related effects of shock waves, radiation and temperature). It is worth noting,

that in the case of evaporation, ozone appears before nitrous oxide due to its lower boiling temperature; at the same time, in the case of explosion, both O_3 and N_2O peaks have left shoulder indicating first evaporation of the existing molecules followed by their generation during the explosion.

In order to estimate the energy density of the produced material, we have performed fast shadow imaging of the explosions using an arc lamp as a source of back light and a Phantom Miro M310 high-speed camera. For that, liquid nitrogen was treated together with 50 mg of either crushed activated carbon or Diaion HP-20 for 30 minutes. After the treatment, out of ~100 ml of leftover liquid, several samples of ~20 ml of solution was placed in aluminum dish (diameter of 73 mm) and let heat up at room temperature conditions. Explosion event was recorded at rates of 15,000 – 20,000 fps, and images of shock wave position were analyzed frame-by-frame using ImageJ software (Figure 23). Using a simplified equation for propagation of a spherical shock wave from a point explosion [15] $D = \left[\frac{3}{4\pi} \times \frac{(\gamma-1)(\gamma+1)^2}{3\gamma-1}\right]^{\frac{1}{2}} \left(\frac{E}{\rho}\right)^{\frac{1}{2}} R^{-\frac{3}{2}}$, where D is shock wave velocity, R – distance from the center, E – energy of the explosion, ρ – gas density and γ – adiabatic index, we have estimated the explosion energy of the produced material to be 110±30 J (Figure 23). In a separate set of experiments, for the same treatment conditions and amounts of treated material, weight of the material was video recoded before and after the explosion in a loosely closed volume (to prevent loss of the adsorbent while generated gases were allowed to escape) using Fisher Scientific Accu-64 analytical balance. Using this technique, we estimate the weight of the exploded material to be 8.2±2.1 mg – this includes all materials that was lost, including ozone which we estimate to be few ppm (from the FTIR measurements reported above), or ~10^{-8} mg. Therefore, we can estimate total energy density of the material produced by nanosecond-pulsed spark in liquid nitrogen to be about 13.3±3.5 kJ/g, or 3.2±0.8 in TNT (energy density 4.1 kJ/g) equivalent, which is close to predicted number for polymeric nitrogen network of ~11.3 kJ/g and higher than that for *cg*-N (9.7 kJ/g) [1]. To compare, energy density of ozone is only 2.9 kJ/g.

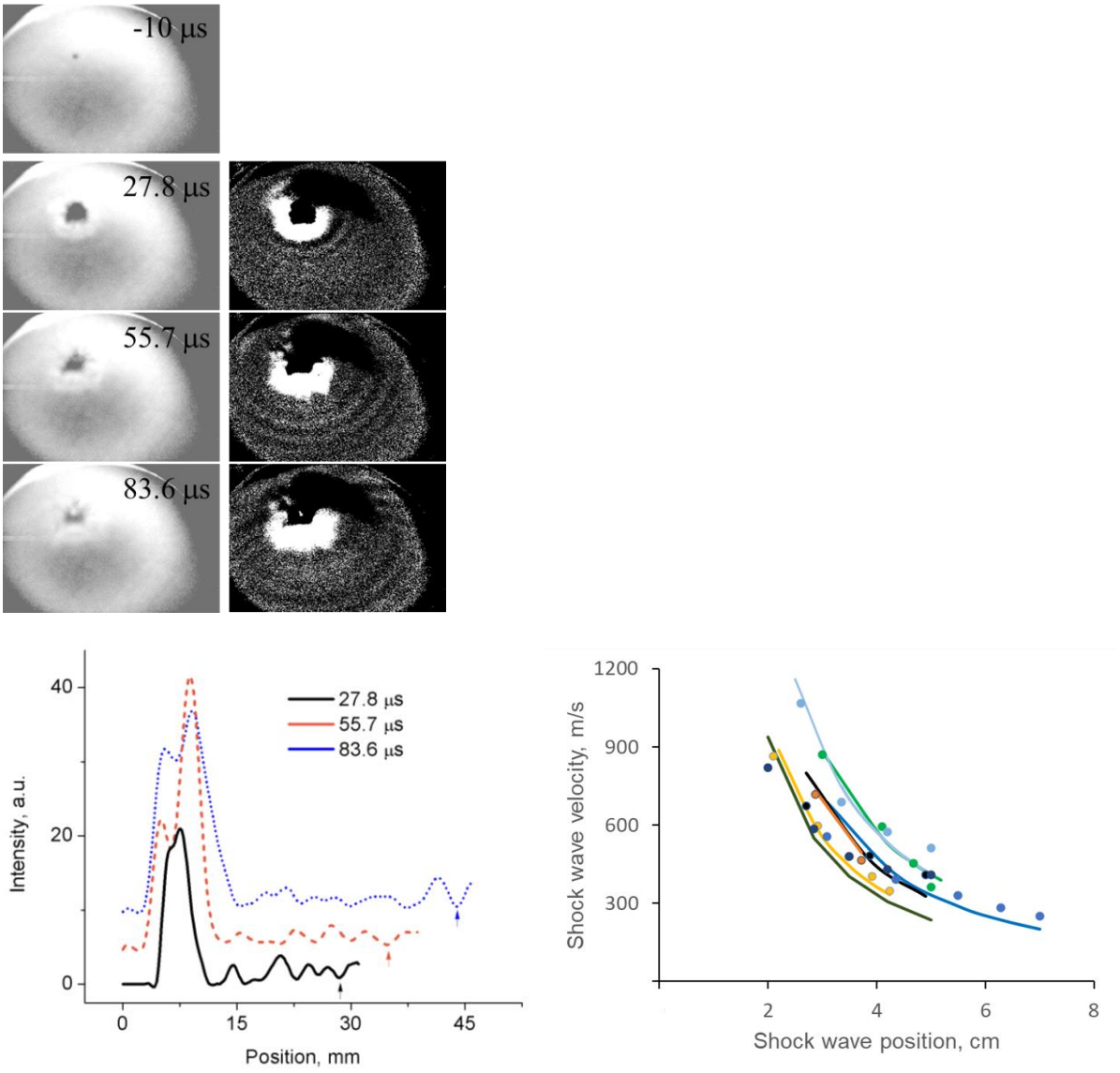

Figure 23. Original and ImageJ-enhanced fast-camera captured frames of the explosion video of plasma-treated liquid nitrogen in presence of activated carbon for shock wave imaging (top). Extracted from images above pixel intensity profiles showing position of the shock wave from the center of explosion (bottom left). Measured from the images (markers) and calculated (solid lines) shock wave propagation velocities as a function of the distance from the explosion center for several different experiments (bottom right).

Using experimental techniques, we have shown:

1. Nanosecond-pulsed spark plasma treatment of liquid nitrogen results in generation of fluorescent material, which closely resembles Raman spectra of amorphous nitrogen previously obtained using high pressure compression of molecular nitrogen. The fluorescence disappears at temperature around -150 °C. The material exhibits unstable properties when heated, however explosions are poorly reproducible.
2. Addition of adsorbents with characteristic pore sizes of >5 nm (indicating that only relatively large molecules being adsorbed) allows reproducible recovery of the produced

material and its explosion upon heating. Fluorescence of in the Raman spectra of the physisorbed material completely disappears at around -120 °C.

3. Similar to our previous study with nanosecond-pulsed corona treatment of liquid nitrogen, FTIR measurements of the sample decomposition via evaporation compared to its explosion in air reveal generation of only ozone and nitrous oxide (while no other NO_x species were detected) which are believed to be generated via electronically excited nitrogen produced during the polynitrogen decomposition.
4. Shadow imaging of the shock wave propagation from the exploded material allowed us to estimate its energy density to be about 13.3±3.5 kJ/g (3.2±0.8 in TNT equivalent), close to predicted number for polymeric nitrogen network of ~11.3 kJ/g.

It must be noted, that obtained material may be (however, unlikely) related to generation of metal- or carbon-containing compounds (material from the eroded electrode), for example, Fe-N systems, which estimated energy densities are about twice that of TNT and suggested to be metastable down to ambient pressures [40].

8. In-liquid nanosecond-pulsed spark discharge plasma: Synthesis of polynitrogen from potassium azide in liquid nitrogen

Here we report a method about synthesis of polynitrogen materials by nanosecond-pulsed spark discharge plasma under liquid nitrogen. In-liquid nanosecond-pulsed spark discharge plasma is a potential method for unconventional high energy material generation, based on the combination of 1) energetic property of discharge itself and 2) low temperature highly compressed liquid nitrogen surroundings. The polynitrogen material was synthesized from potassium azide, preliminarily characterized by Raman and FTIR spectroscopy, as K_2N_6, with planar N_6 rings and K^- ions having P6/mmm symmetry. The mechanism of such transformation was determined as being in contact with the spark discharge, that is, due to the highly unstable short life active species formed in plasma channel or novel high temperature of the nanosecond-pulsed spark discharge itself.

Alkali metal azides such as sodium azides are widely used as precursors for generation of polynitrogen materials, based on their behaviors under extremely high pressure. High pressure phase transitions have also been reported in rubidium azide (RbN3), cesium azide (CsN3), and thallium azide (TlN3) with relatively low transition pressures (<1 GPa) [41]. With compression, they would have structural phase transitions involving lattice distortions together with direction change or polymerization of the linear azide anions [42].

Alkali metals can also stabilize charges that leftover after the polymeric nitrogen material formation [43]. In our previous work, sodium azide was used as precursor for generation of high energy density polynitrogen N_6 materials. Unlike sodium azide which has $C_2/_m$ symmetry, potassium azide has $I4/_{mcm}$ symmetry at room temperature. With different precursor crystal

structure, it is possible to synthesize polynitrogen materials with different structures. In our study, we report the nanosecond-pulsed spark discharge treatment of potassium azide under liquid nitrogen, and the optical characterizations including FTIR and Raman spectroscopy of the product. We show that plasma treatment results in generation of a new compound identified as K_2N_6 with planar N_6 rings having $P_6/_{mmm}$ crystal symmetry.

The experiments were done in the following setup: two stainless steel pins with about 100 μm tip curvature were fixed on separate metal rods at a distance about 0.1 mm for generation of spark discharge. The metal rods were fixed on the lid of a 450 ml double-walled glass flask. Potassium azide powder was placed at the bottom of the flask. The distance between the discharge and potassium azide powder was adjustable.

Spark discharge pulses were generated by a FPG 20-05NM high voltage power supply (FID Technology) which can provide pulses with maximum amplitude of 20 kV and duration (90% amplitude) of 10 ns. 10.5 kV amplitude was used in all the experiments reported in this paper. Spark discharge pulses were delivered by the power supply to the needle electrodes via a 6 m long RG393/U 50 Ω high voltage coaxial cable.

Industrial grade liquid nitrogen (Airgas) was used in all experiments. Approximately 1 g potassium azide powder (Sigma) was treated by spark discharge under liquid nitrogen inside 450 ml double-walled glass chamber. Potassium azide powder did not dissolve in liquid nitrogen and stayed in powder form at the bottom of the chamber.

Fourier transform infrared spectroscopy (FTIR) measurements were done by a Nicolet 8700 FTIR spectrometer. Samples were placed in between two pieces of KBr windows (25 *4 mm, Pike Technologies) and the windows were fixed in a sample holder (ThermoFisher). The assembly was done under liquid nitrogen and measurements were done right after the holder being transferred to the spectrometer. Nitrogen gas (Airgas) was used to purge the sample holder chamber to avoid CO_2 and H_2O depositing on the window.

Raman spectra were measured using a Princeton Instruments-Acton Research TriVista TR555 spectrometer system together with a SDM532-100SM-L Newport 532 nm Spectrum Stabilized Laser Module and RPB532 Raman probe (InPhotonics). Measurements were done inside a glove box purged with compressed air to avoid humidity (Liquid nitrogen has a boiling point of about −195.8 °C, water and carbon dioxide in air would deposit at the surface of powder being measured). Samples were placed at the top of a metal sample holder inside a CG-1592-03, Chemglass Life Sciences liquid nitrogen Dewar. Raman spectrum was obtained from underneath few mm liquid nitrogen layer on top of the sample.

The treatments of approximately 1 g of potassium azide powder were done inside the 450 ml double-walled glass chamber under liquid nitrogen for a duration of 30 minutes with different powder-to-discharge distances. The distance between the powder and discharge was set to range of 0-20 mm, the distance of 0 represented that the discharge was in contact with powder. The color of potassium azide powder changed from transparent to lilac after the plasma treatment for distances less than 20 mm and the shorter the distance the more obvious color change was obtained. At setup with 20 mm discharge-to-powder distance the color of treated potassium azide just turned

to dark grey. To eliminate the effect of the low temperature caused by liquid nitrogen, potassium azide powder was stored under liquid nitrogen for 30 minutes, no color change was observed. Explosion test was also done to the treated samples, by pouring the sample together with liquid nitrogen directly into a metal dish to generate rapid temperature change. Unlike the previous works with porous adsorbent materials, the powder did not explode.

FTIR Spectrum

We recorded the FTIR spectrum of the untreated and treated potassium azide from all setups. The obtained spectrum is shown in Figure 24, the new peaks formed after the spark discharge treatment are labeled. The spark discharge treated potassium azide powder was fixed between two KBr windows, and the windows were slotted in a sample holder. The assembly was done under liquid nitrogen and the deposition of CO_2 on the surface of the window resulted in the negative region on the FTIR spectrum (650 and 2200 cm^{-1}). New peaks located at 464 cm^{-1}, 555 cm^{-1}, 613 cm^{-1}, 678 cm^{-1}, 703 cm^{-1}, 840 cm^{-1}, 1056 cm^{-1}, 1184 cm^{-1}, 1214 cm^{-1}, 1384 cm^{-1}, 1465 cm^{-1}, 1654 cm^{-1} and 2057 cm^{-1} were formed after 30 min spark discharge treatment of potassium azide under liquid nitrogen. The set of new peaks only showed up in the discharge-to-powder distance of 0, which means the contact of discharge and the material is essential to such transformation.

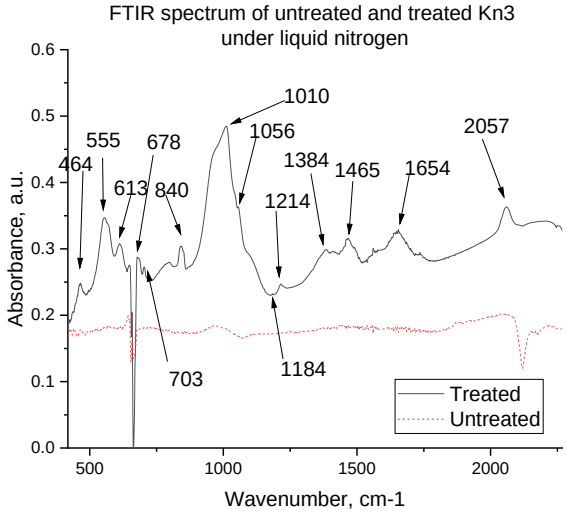

Figure 24. FTIR spectrum of potassium azide with/without spark discharge treatment

A set of new peaks were formed after the treatment, which indicates potential structure change. To assign these set of new peaks, we compared them with the PW91 DFT calculation predicted high-pressure product vibrational modes listed in Table 4 [44].

Table 4. List of calculated IR vibrational frequencies of D_2 hexaazabenzene molecule compared with observed frequencies

Molecular structure	Symmetry	calculated IR frequency, cm^{-1}	Observed IR frequency, cm^{-1}
D2 Hexaaza-benzene			
	B3	588.5	555
	B2	710.4	703
	B3	872.3	840
	B1	1002.8	1010
	B3	1184.3	1184

The obtained FTIR spectrum showed good correspondence with the predicted structure, thus one of the products obtained by nanosecond-pulsed spark discharge plasma treatment of potassium azide under liquid nitrogen can be identified as K_2N_6 with $P6/_{mmm}$ symmetry and planar D_2 N_6 hexaazabenzene rings locating on the corner of the crystal. Additional peaks can be assigned to other polynitrogen materials, or mixture of multiple structures [45], neutral or single negatively charged N_6 would also be formed in the process leaving vacancies being occupied by electrons, hence induced color change.

Color change

The color change of potassium azide from transparent to lilac suggested electronical structure change by 30 min treatment of nanosecond-pulsed spark discharge. The lilac color shows correspondence with the color of color center formation in potassium chloride [46]. A color center (also called as F-center or Farbe center) is a kind of crystal defect where unpaired electrons taking over the position of anionic vacancies [47]. The electrons absorb light in visible region and turn the material from transparent to colored [48]. The color resulted from color center can be applied to identify salts, based on the dependence of metal cations [49]. Ionizing radiation is a resulting factor for color centers [50]. Higher energy ultraviolet part of the electromagnetic spectrum is a part in our spark discharge plasma, such kind of ionic radiation can be applied to explain the formation of color center in our case. As noticed, shorter powder-to-discharge caused significant color change. The intensity of UV radiation is proportional to the reciprocal of distance square, which suggests that UV intensity is highly dependent on distance. Therefore, the color change is UV-induced and distance dependent.

Raman Spectrum

In Raman spectra measurements, after 30 min treatment all the powders were moved under liquid nitrogen into the heavy metal sample holder to ensure mild temperature rise. The Raman spectrum of both untreated and treated potassium azide are shown in Figure 25. The Raman spectrum of

untreated potassium azide was also obtained under liquid nitrogen to avoid potential structure change arose from liquid nitrogen temperature. In the 20 mm distance setup, several new peaks formed after 30 min treatment under liquid nitrogen: 326cm^{-1}, 630 cm^{-1}, 937 cm^{-1}. For shorter distance setup two additional peaks located at 1235 cm^{-1} and 1523 cm^{-1} appeared.

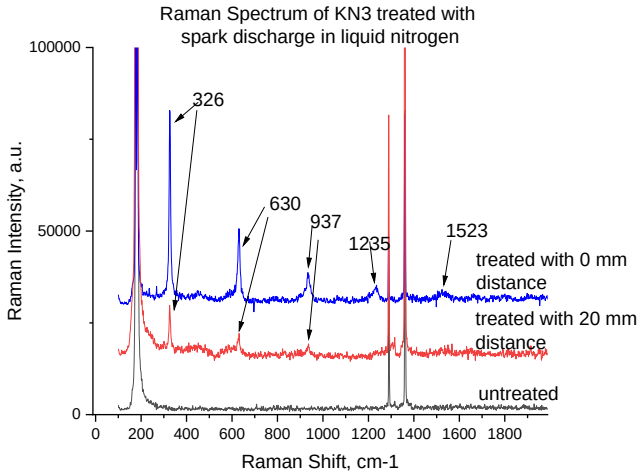

Figure 25. Raman spectrum of potassium azide with/without spark discharge treatment

Potassium azide has crystal structure with $I4/_{mcm}$ symmetry at ambient condition, Raman peaks located at 147 cm^{-1}, 1268 cm^{-1} and 1340 cm^{-1} correspond to the R, v_1 and $2v_2$ vibration of potassium azide [51]. As noticed the set of new peaks are located with nearly same shift offset, which can be assigned as overtone or fermi resonance of the crystal liberational mode. The position of the main new peak 327 cm-1 corresponds to the high-pressure potassium azide product [52]. The predicted polynitrogen structure in potassium azide has crystal structure at $p6/_{mmm}$ symmetry and N_6 planar ring structure at corner position. The predicted Raman peaks for planar N_6 is shown in shown low intensity [23]. We compared our Raman spectrum with another crystal with $p6/_{mmm}$ symmetry Li_3N [32], the main peak position and overtones showed good correspondence.

Mechanism study of color change, crystal structure change and polymerization

Nanosecond-pulsed spark discharge plasma release energies to liquid nitrogen during the treatment through very complex dynamic processes. In our case, to investigate the functioning factor that caused polymerization of nitrogen in potassium azide after nanosecond-pulsed spark discharge, few more setups were made by isolating potassium azide powder from the liquid nitrogen with different materials.

In our reaction system, several factors are needed to be considered as the resulting factor of color change, crystal structure change and polymerization. Based on our Raman spectrum, crystal structure change did not differ a lot with longer distance between discharge and powder, thus relatively stable active species would be possible to be considered as a possible factor. UV radiation and electric field generated by nanosecond-pulsed spark discharge are also factors to be considered. The setups with same discharge-to-powder distance set as 10 mm inside the glass chamber that built were: 1) with two pieces of quartz covered. 2) with metal mesh covered. 3) with

both quartz and metal mesh covered. 4) with plastic tube covered. 5) with two pieces of glass covered. All the setups can separate the powder from liquid nitrogen. Quartz can let certain wavelength UV, Visible light, and IR to go through. Metal mesh is a conductor, and the electric field is zero inside a conductor. Plastic and glass are used to block both active species and UV. Table 5 showed the detailed information of mechanism study. Color change was checked by visualization, crystal structure change was characterized by the appearance of Raman peak located at 326 cm^{-1}, polymerization was determined by the appearance of same set of new peaks as the non-isolated potassium azide FTIR spectrum. The color turned to lilac for setup 1,2 and 3, stayed white for setup 4 and 5. In setup 1 to 3 same Raman peak located at 326cm-1 suggesting crystal structure change were found, in setup 4 and 5 such peaks were not detected. To detect the effect of solely active species, experiments were also done on adding potassium azide into the plasma-treated liquid nitrogen. No color change or crystal structure change or polymerization were observed.

FTIR spectrum were done on all the samples mentioned above. The peaks in FTIR spectrum located at 464 cm^{-1}, 555 cm^{-1}, 613 cm^{-1}, 678 cm^{-1}, 703 cm^{-1}, 840 cm^{-1}, 1056 cm^{-1}, 1184 cm^{-1}, 1214 cm^{-1}, 1384 cm^{-1}, 1465 cm^{-1}, 1654 cm^{-1} and 2057 cm^{-1} suggesting polymerization of nitrogen only occurred under the circumstances of discharge-to-powder distance equals to zero, which means polymerization is arose from contact of potassium azide and the nanosecond-pulsed spark discharge. The functioning factor of polymerization can then be concluded as the several thousand high temperature of the discharge itself or the short-lived unstable active species within the discharge.

It is shown that the color change and crystal structure change were mainly caused by UV radiation, and the polymerization of nitrogen was resulted in the contact with spark discharge. The high temperature of discharge can give energy higher than the transition energy barrier, also the fast quenching can be functioned as stabilization in our case. Obviously, more studies should be done to investigate the detailed mechanism of the polymerization.

Table 5. Experimental information for mechanism study

Setup	Filter material used	Factors eliminated	Factors in function	Color change	Crystal structure change	Polymerization
0	Nothing		Active species, Electric field, UV, Visible light, IR	Yes	Yes	Yes
1	Quartz	Active species	UV, Electric field, Visible light, IR	Yes	Yes	No
2	Mesh	Electric field	Active species, UV,	Yes	Yes	No

			Visible light, IR			
3	Quartz and Mesh	Active species, Electric field	UV, Visible light, IR	Yes	Yes	No
4	Plastic tube	Active species, UV	Electric field, Visible light	No	No	No
5	Glass	Active species, UV	Electric field, Visible light, IR	No	No	No

The optical measurements support the hypothesis that in-liquid nanosecond-pulsed spark discharge induced crystal and structural transformations in potassium azide, and possibly results in polymerization of nitrogen with probable product of N_6 rings. The obtained product is assigned as the same as high-pressure product of potassium azide but due to the huge pressure difference it is hard to verify. The mechanism behind this transformation can be contributed by the effects of plasma radiation. Further studies are needed for different characterizations or synthesis from such azide precursors.

References

1. Dobrynin D, Seepersad Y, Pekker M, Shneider M, Friedman G and Fridman A 2013 Non-equilibrium nanosecond-pulsed plasma generation in the liquid phase (water, PDMS) without bubbles: fast imaging, spectroscopy and leader-type model J. Phys. D: Appl. Phys. 46 105201
2. Seepersad Y, Nanosecond Pulsed Discharge in Water without Bubbles: A Fundamental Study of Initiation, Propagation and Plasma Characteristics, PhD Thesis, Drexel University, USA
3. Seepersad Y, Pekker M, Shneider M N, Fridman A and Dobrynin D 2013 Investigation of positive and negative modes of nanosecond pulsed discharge in water and electrostriction model of initiation J. Phys. D: Appl. Phys. 46 355201
4. Lesaint 2016 Prebreakdown phenomena in liquids: propagation 'modes' and basic physical properties *J. Phys. D: Appl. Phys.* 49 144001
5. Frayssines P E, Bonifaci N, Denat A and Lesaint O 2002 Streamers in liquid nitrogen: characterization and spectroscopic determination of gaseous filament temperature and electron density J. Phys. D: Appl. Phys. 35 369–77
6. *Starikovskiy A, Yang Y, Cho Y I and Fridman A 2011 Non-equilibrium plasma in liquid water: dynamics of generation and quenching Plasma Sources Sci. Technol. 20 024003*
7. Pongrác B, Šimek M, Ondáč P, Člupek M, Babický V and Lukeš P 2019 Velocity of initial propagation of positive nanosecond discharge in liquid water: dependence on high voltage amplitude and water conductivity *Plasma Sources Sci. Technol.* 28 02LT02
8. Yamazawa K and H Yamashita 1997 Prebreakdown Density Change Streamer in Liquid Nitrogen Jpn. J. Appl. Phys. 36 6437
9. Laux C O 2002 Radiation and nonequilibrium collisional-radiative models Physico-Chemical Modeling of High Enthalpy and Plasma Flows (von Karman Institute Lecture Series 2002-07) ed D Fletcher et al (Belgium: Rhode-Saint-Genese)
10. M. I. Eremets, R. J. Eremets, and H.-k. Mao, 2001 Semiconducting non-molecular nitrogen up to 240 GPa and its low-pressure stability, Nature, 411, 170–174 (2001).
11. Goncharov A F, Gregoryanz E, Mao H-K, Liu Z, and R J Hemley 2000 Optical Evidence for a Nonmolecular Phase of Nitrogen above 150 GPa Phys. Rev. Lett. 85, 1262
12. Gregoryanz E, Goncharov A F, Hemley R J and H-K Mao 2001 High-pressure amorphous nitrogen Phys. Rev. B 64, 052103
13. Gregoryanz E, Goncharov A F, Hemley R J, Mao H-K, Somayazulu M and G Shen 2002 Raman, infrared, and x-ray evidence for new phases of nitrogen at high pressures and temperatures Phys. Rev. B 66, 224108
14. Olijnyk H and A P Jephcoat 1999 Vibrational Dynamics of Isotopically Dilute Nitrogen to 104 GPa Phys. Rev. Lett. 83, 332
15. Wu, Z. , Benchafia, E. M., Iqbal, Z. and Wang, X. (2014), N_8^- Polynitrogen Stabilized on Multi-Wall Carbon Nanotubes for Oxygen-Reduction Reactions at Ambient Conditions. Angew. Chem. Int. Ed., 53: 12555-12559
16. I A Kossyi et al Kinetic scheme of the non-equilibrium discharge in nitrogen-oxygen mixtures, Plasma Sources Sci. Technol. 1 207, 1992
17. Peiris S M and T P Russell 2003 Photolysis of Compressed Sodium Azide (NaN3) as a Synthetic Pathway to Nitrogen Materials The Journal of Physical Chemistry A 2003 107 (6), 944-947
18. Isokoski K, Poteet C A and Linnartz H, 2013, Highly resolved infrared spectra of pure CO2 ice (15–75 K), Astronomy and Astrophysics 555 A85
19. L Brewer 1972 Infrared Absorption Spectra of Isotopic Ozone Isolated in Rare-Gas Matrices J. Chem. Phys. 56, 759

20. L. Schriver-Mazzuoli et al 1995 Ozone generation through photolysis of an oxygen matrix at 11 K: Fourier transform infrared spectroscopy identification of the O...O3 complex and isotopic studies J. Chem. Phys. 102, 690
21. A Lakhlifi et al 1993 Interpretation of the infrared spectrum of ozone trapped in inert matrices Chem Phys 177 31-44
22. B D Teolis et al 2007 Low density solid ozone J. Chem. Phys. 127, 074507
23. R D Bartlett et al Stable polynitrogen molecules from N_2 to N_{10} and their anions and cations IR vibrational frequencies and intensities, http://www.qtp.ufl.edu/~bartlett/downloads/polynitrogen.pdf
24. M Tobita and R J Bartlett 2001 Structure and Stability of N_6 Isomers and Their Spectroscopic Characteristics J. Phys. Chem. A 105 16 4107-4113
25. Benchafia et al 2017 Cubic gauche polymeric nitrogen under ambient conditions, Nature Communications, vol 8, Article number: 930
26. N Holtgrewe et al 2016 Photochemistry within Compressed Sodium Azide J. Phys. Chem. C, 120, 28176−28185
27. S Duwal et al 2018 Transformation of hydrazinium azide to molecular N8 at 40 GPa J. Chem. Phys. 148, 134310
28. Benchafia et al 2017 Cubic gauche polymeric nitrogen under ambient conditions, Nature Communications, vol 8, Article number: 930
29. Eremets M I et al 2004 Single-bonded cubic form of nitrogen Nat. Mater., 3, 558–563
30. Laniel D, Dewaele A and Garbarino G 2018 High Pressure and High Temperature Synthesis of the Iron Pernitride FeN2, Inorg. Chem. 57 6245−6251
31. Christe, K.O., Wilson, W.W., Sheehy, J.A. and Boatz, J.A. (1999), N_5^+: A Novel Homoleptic Polynitrogen Ion as a High Energy Density Material. Angewandte Chemie International Edition, 38: 2004-2009.
32. Moran Noyman, Shmuel Zilberg, and Yehuda Haas, J. Phys. Chem. A 2009, 113, 7376–7382
33. T. Zhang, S. Zhang, Q. Chen, and L.-M. Peng, PHYSICAL REVIEW B 73, 094105 2006
34. Hakima Abou-Rachid, Anguang Hu, Vladimir Timoshevskii, Yanfeng Song, and Louis-Simon Lussier Nanoscale High Energetic Materials: A Polymeric Nitrogen Chain N8 Confined inside a Carbon Nanotube Phys. Rev. Lett. 100, 196401
35. Benchafia, E.M., Yao, Z., Yuan, G. *et al.* Cubic gauche polymeric nitrogen under ambient conditions. *Nat Commun* **8,** 930 (2017)
36. Hitesh Sharma, Isha Garg, Keya Dharamvir, and V. K. Jindal, J. Phys. Chem. C 2010, 114, 9153–9160
37. Feng Peng, Yansun Yao, Hanyu Liu, and Yanming Ma The Journal of Physical Chemistry Letters 2015 6 (12), 2363-2366
38. Zhang, J., Wang, X., Yang, K. *et al.* The polymerization of nitrogen in Li_2N_2 at high pressures. *Sci Rep* **8,** 13144 (2018)
39. M. J. Lipp, J. Park Klepeis, B. J. Baer, H. Cynn, W. J. Evans, V. Iota, and C.-S. Yoo Transformation of molecular nitrogen to nonmolecular phases at megabar pressures by direct laser heating Phys. Rev. B 76, 014113
40. Bykov, M., Bykova, E., Aprilis, G. et al. Fe-N system at high pressure reveals a compound featuring polymeric nitrogen chains. Nat Commun 9, 2756 (2018).
41. Pistorius, C. W. 1969 *J. Chem. Phys.* **51(6)**, 2604-2609
42. Wang Q, Ma Y, Sang D, et al. 2018, *[J]. Applied Physics Letters,* **112(17)**: 173903
43. Williams A S, Steele B A, Oleynik I I. 2017, *[J]. The Journal of chemical physics,* **147(23)**: 234701

44. Noyman M, Zilberg S, Haas Y. 2009, *[J]. The Journal of Physical Chemistry A*, **113(26)**: 7376-7382
45. Workentin M S, Wagner B D, Negri F, et al. 1995, *[J]. The Journal of Physical Chemistry*, **99(1)**: 94-101
46. Maycock J N. 1964, *[J]. Journal of Applied Physics,* **35(5)**: 1512-1515.
47. Tilley R J D. 2008. *Defects in solids[M]*. John Wiley & Sons
48. Nassau K. . 2001.*The physics and chemistry of color: the fifteen causes of color[M]*
49. Hayes W, Stoneham A M. 1985, *Wiley[J]. New York,.*
50. Hersh H N. 1966, *[J]. Physical Review*, **148(2)**: 928
51. Bryant J I, Brooks III R L. 1965, *[J]. The Journal of Chemical Physics,* **43(3)**: 880-882
52. Ji C, Zheng R, Hou D, et al. 2012, *[J]. Journal of Applied Physics*, **111(11)**: 112613.